Basic guidelines for nuclear power reactor monitoring using neutron noise analysis

by

Kenneth Eugene Howard

A Thesis Submitted to the
Graduate Faculty in Partial Fulfillment of
The Requirements for the Degree of
MASTER OF SCIENCE

Department: Chemical Engineering and Nuclear Engineering
Major: Nuclear Engineering

Signatures have been redacted for privacy

Iowa State University
Ames, Iowa

1978

TABLE OF CONTENTS

LIST OF TABLES

LIST OF FIGURES

I. INTRODUCTION

The nuclear industry is required by federal regulations and its own drive for maximum efficiency to maintain an unquestionably high level quality assurance (QA) program. Conventional QA testing methods are sufficient for components and procedures outside of reactor operation. The hostile environment of the reactor core makes continued quality assurance monitoring difficult. The monitoring activity requires operational testing, and a technique used extensively for this type of testing is the study of randomly fluctuating variables. These time varying fluctuations are termed reactor noise. Noise analysis is the statistical analysis of the noise to: a) extract information about characteristics of the system and b) function as a diagnostic tool (22). The random fluctuations of interest in this study represent fluctuations in the neutron flux caused by coolant flow variations, vibration of core components, and global reactivity effects (23) and are termed neutron noise. Neutron noise analysis has several advantages in the area of operational testing (24):

1. There is essentially no disturbance of reactor operation.
2. Existing instrumentation and equipment can be used.
3. Information can be obtained which cannot be obtained from other testing techniques.

Neutron noise analysis can provide a higher level of assurance that the core's mechanical and hydraulic design integrity is being maintained. This better understanding of the core's integrity can provide two benefits:

1. Incipient component failures can be detected and possibly corrected before a forced shutdown occurs.

2. Wasteful deratings due to inadequate information can be avoided.

The added knowledge of the core's performance during operation can be used to improve the design of future components or systems.

Government regulatory agencies have used noise analysis in the past and may require its use in the future. In 1975 the Nuclear Regulatory Commission (NRC) required nine utilities to provide information about abnormal in-core vibrations (1). In 1969, the Advisory Committee on Reactor Safeguards (ACRS) initiated a requirement for nuclear power plants to have a monitoring system for vibrations and loose parts. Neutron noise analysis can provide essential information in the detection of abnormal vibrations.

Despite these favorable points of neutron noise analysis the nuclear power industry continues to be hesitant to use neutron noise analysis because of inadequate baseline data. A very important issue is the legal responsibility of a utility to shut down a reactor, thereby incurring substantial financial losses, when neutron noise analysis indicates a change in reactor conditions not correlated with other variables being monitored or reduced performance of the reactor. The present state-of-the-art cannot adequately address this issue. Actual reactor experience with neutron noise analysis is needed to provide some insight into this issue.

The objectives of this study are:

1. A neutron noise data acquisition system will be developed.

2. The data acquisition system will be tested in an operating power reactor.

3. The amount of data required to establish a noise signature pattern (NSP) will be determined.

4. The length of time a NSP is valid will be indicated.

5. A reactor monitoring system using neutron noise analysis will be proposed and tested.

II. LITERATURE REVIEW

The techniques for utilizing neutron noise analysis have been firmly established, but little experience has been gained with power reactors. Analysis in the frequency domain has been proven to be very useful and will be used in this study (14). Methods for data acquisition have been described by Fry et al. (8), Fry et al. (9), and Lewis et al. (15). Techniques for data analysis have been developed by Gonzalez et al. (11) and Piety and Robinson (21). Data acquisition and analysis techniques used in the present study were strongly affected by the work done by Holthaus (13).

Commercially available equipment for data acquisition and analysis was found to be cost prohibitive (5, 8). Therefore, existing data analysis equipment (19) was used and data acquisition equipment was built.

Neutron noise analysis has been used successfully on a number of reactors and has been used routinely at the Trino Reactor (26). Lewis et al. (15) obtained noise signature patterns during startup physics testing and approach to full power at the Duke Power Company's Oconee I. Neutron noise analysis has been used by Fry et al. (8) to detect core barrel motion at the Consumers Power Company's Palisades Nuclear Plant. Mott et al. (18) and Harris (13) have used neutron noise analysis to detect the vibration and impacting of instrument tubes in BWR-4's. Fry (10) used neutron noise analysis to detect plugged off-gas lines at the MSRE and failures of both upper and lower control rod bearings at the HFIR.

III. THEORY

A. Frequency Domain Analysis

Neutron noise analysis is the statistical analysis of noise data to extract useful information about the operating conditions of reactor internal components. Noise data in the time domain are often transformed to the frequency domain. The transformation from the time to the frequency domain is accomplished by using the fast Fourier transform (FFT) (6, 14) which is a digital computer algorithm for the calculation of Fourier transforms. Two important considerations in the use of the FFT is the window function applied to the data and the sampling frequency of the data in the time domain (4). The results of this transformation are the real and imaginary parts of a function termed power spectral density (PSD), which is the distribution of noise power as a function of frequency. The real and imaginary parts are used to form the PSD, shown in Appendix B.

The FFT has been applied to a wide range of reactor noise and this experience has firmly established the FFT and the resulting PSD as valuable noise analysis techniques. The noise signals are often analyzed in pairs to obtain a cross power spectral density (CPSD). CPSD's give the noise power distribution as a function of frequency which eliminates the noise that is not common (uncorrelated) to both detectors. A measure of the closeness of the cause-and-effect relationship between two detectors is coherence. Another useful relationship between two detectors is the phase lag which can be converted into a time lag and used to calculate the coolant void velocity in the core.

B. At-Power Reactor Noise

The power spectral density (PSD) observed using a fission chamber in a power reactor is given by (10)

$$\Phi_N(\omega) = \frac{2W_n Q^2 P}{\Lambda} + \frac{W_n^2 Q^2}{\Lambda^2} |G_o(\omega)|^2 [\Phi_S(\omega) + P^2 \Phi_\rho(\omega)] \qquad (1)$$

where the first term is the white-noise from the detection process, the second term is due to internal noise and the last term is the external reactivity term. The external noise is caused by component vibrations, coolant void formation, and reactivity feedback effects. Q is the charge transferred per neutron absorbed, W_n is the detector efficiency, Λ is the neutron generation time, P is the reactor power level and G_o is the zero power reactivity transfer function. Cohn (7) has shown $\Phi_S(\omega)$ to be proportional to P. Therefore, at the power levels in question, at least several hundred MW, the external reactivity noise, $\Phi_\rho(\omega)$ is the dominant term and

$$\Phi_N(\omega) \simeq \frac{P^2 W_n^2 Q^2}{\Lambda^2} |G_o(\omega)|^2 [\Phi_\rho(\omega)]. \qquad (2)$$

Also, the average detector current I_{dc} is

$$I_{dc} = \frac{PW_n Q}{\Lambda} . \qquad (3)$$

The voltage signal, V_{dc}, from which the data were taken is proportional to I_{dc}. Therefore,

$$\Phi_N(\omega) \propto V_{dc}^2 |G_o(\omega)|^2 [\Phi_\rho(\omega)]. \qquad (4)$$

When the observed PSD is normalized, divided by V_{dc}^2, the PSD will be independent of power level. Furthermore, this normalization will account for the efficiency and sensitivity of the detector and the preamplifier gain. This normalization allows spectra from different detectors and even different reactors of the same standard design to be compared on the same absolute scale. $G_o(\omega)$ is approximately a smooth function over the frequency range of interest. Therefore, the PSD obtained from Eq. (4) takes on the shape of the external reactivity spectrum $\Phi_\rho(\omega)$ and the amplifying effect of $|G_o(\omega)|^2$ causes the PSD to be very sensitive to changes in $\Phi_\rho(\omega)$.

Fry et al. (9) have stated the frequency range of interest in BWR noise analysis as 0 to 10 Hz and that this range can be broken into two segments. In the 0 to 2 Hz range global noise dominates and in the 2 to 10 Hz range local noise dominates. The global noise is caused by total core reactivity changes and local noise is caused by coolant void formation and component vibrations. Therefore, loose parts and vibrations monitoring should concentrate on the 2 to 10 Hz frequency range.

C. Frequency Domain Analysis in Power Reactors

Neutron noise analysis in the frequency domain can be broken into three categories (22):

1. Vibration measurements
2. Approach to power monitoring
3. Normal full-power operations.

Vibration measurement is the occasional use of neutron noise when reactor core internals are believed to be behaving abnormally. Neutron noise analysis combined with other noise analysis (pressure, acoustical, etc.) can add very useful information about core internals movements.

Approach to power monitoring is done to establish the background noise of the detectors to be used in full-power monitoring program. This background noise changes when the coolant flow rates, rod positions or core fuel composition changes. Therefore, to use neutron noise analysis for malfunction diagnosis, one must first collect a library of normal neutron noise signature patterns for normal operational conditions of the reactor. These neutron noise patterns are the PSD's and CPSD's discussed earlier. Lewis et al. (15) obtained neutron noise data for Oconee I during startup physics testing and the approach to full power to obtain information about the original noise pattern of the plant.

The detectors monitored in the approach to power program will continue to be monitored at full power. This must be a continuing process for that particular reactor if neutron noise is to be useful for malfunction detection, because even the slightest intentional change of any core component can sometimes change the noise signature pattern (NSP) significantly. Automated data acquisition and analysis becomes very important at this stage of monitoring because most of the reactor's life will be spent in this operational condition. This stage of monitoring is the most useful for surveillance and diagnostics. If a deviation from the normal pattern is detected when there is no accompanying change in operational conditions then a malfunctioning

component is most likely the problem. Even at this point one cannot select a particular component as having failed. All the change in the noise pattern indicates is that something in the core is not functioning normally. This is often very important information for reactor operation.

D. Requirements for Data Acquisition

Noise patterns for normal reactor operation are required for noise analysis to be useful. These normal noise patterns must be obtained from averaging a sufficient number of PSD's. These PSD's must be acquired during the same reactor conditions and time span, which requires data collection several times daily for a period of time sufficient to acquire the required noise patterns. Normalization is required to permit these neutron noise patterns to be used for different reactors of the same design. The normalization consists of dividing the raw PSD by $\overline{V}^2$ and A_T^2, where

$\overline{V}$ = mean voltage of noise data signal

A_T = total gain applied to data acquisition and analysis

and thus, obtaining a normalized power spectral density (NPSD). The collection of enough NPSD's allows the establishment of a noise signature pattern. A noise signature pattern is a NPSD which characterizes a set of reactor operating conditions. It is the values of the noise signature pattern which are used in the detection of abnormal reactor operation. The difference between a NPSD and a noise signature pattern

is that a NPSD is derived from one data record and a noise signature pattern is acquired from averaging a sufficient number of NPSD's.

IV. EXPERIMENTAL PROCEDURES AND EQUIPMENT

A. Data Signal

The neutron noise data studied were taken from Local Power Range Monitors (LPRM's) in the core of the Duane Arnold Energy Center, a 540 MW BWR-4, located at Palo, Iowa. The Duane Arnold Energy Center (DAEC) was one of the BWR-4's that experienced LPRM tube impacting against fuel channels. The bypass coolant holes in the core plate were plugged to reduce coolant flow induced vibrations. To cool the detector, two 9/16" diameter holes were drilled in the lower tie plate to allow a reduced coolant flow. Duane Arnold was at 100% power during most data collection. These LPRM's are composed of vertical strings of four fission chambers spaced regularly throughout the core. The four fission chambers of each LPRM are spaced 18, 54, 90, and 126 inches from the bottom of the core and labeled A, B, C, and D respectively. The signal from each detector is composed of a mean voltage ($\bar{V}$) with a small, fluctuating noise voltage (dv) superimposed upon it, shown in Fig. 1. It is this small noise signal which carries the useful information.

The LPRM string chosen for this study was 40-25, shown in Fig. 2. 40-25 was chosen because all the surrounding control rods were completely withdrawn during all data acquisition.

B. Equipment

The main functions of data acquisition and analysis equipment are:

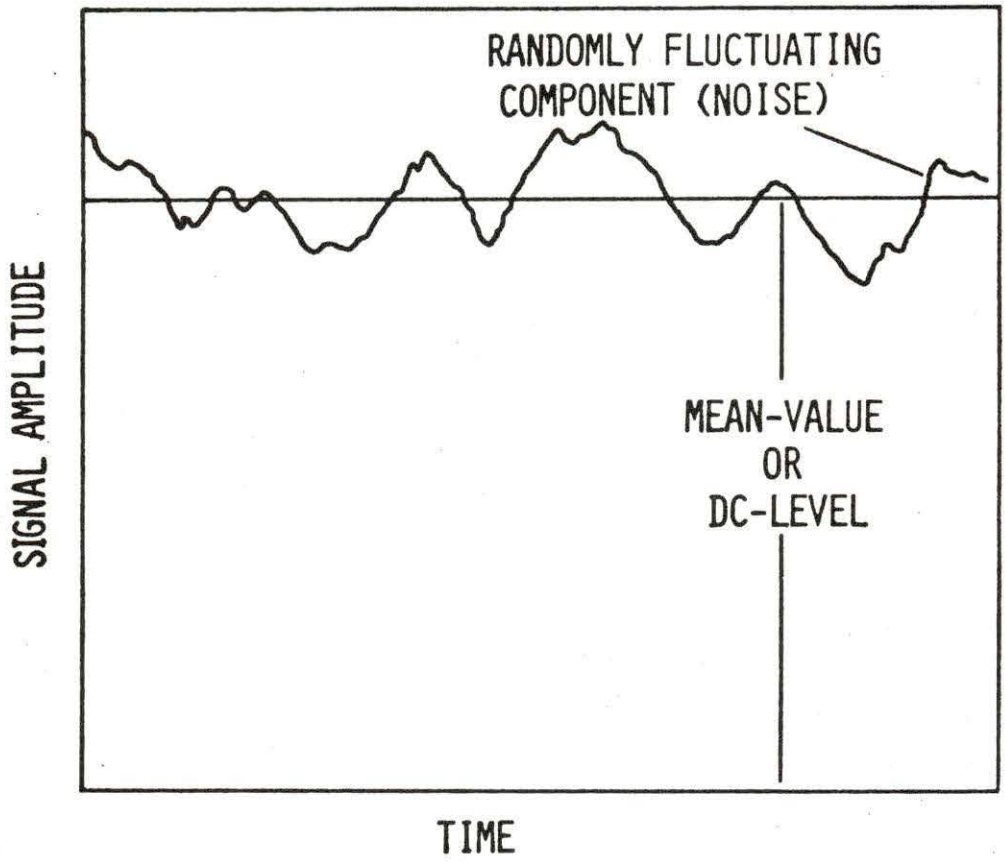

Fig. 1. Components of a neutron sensor signal

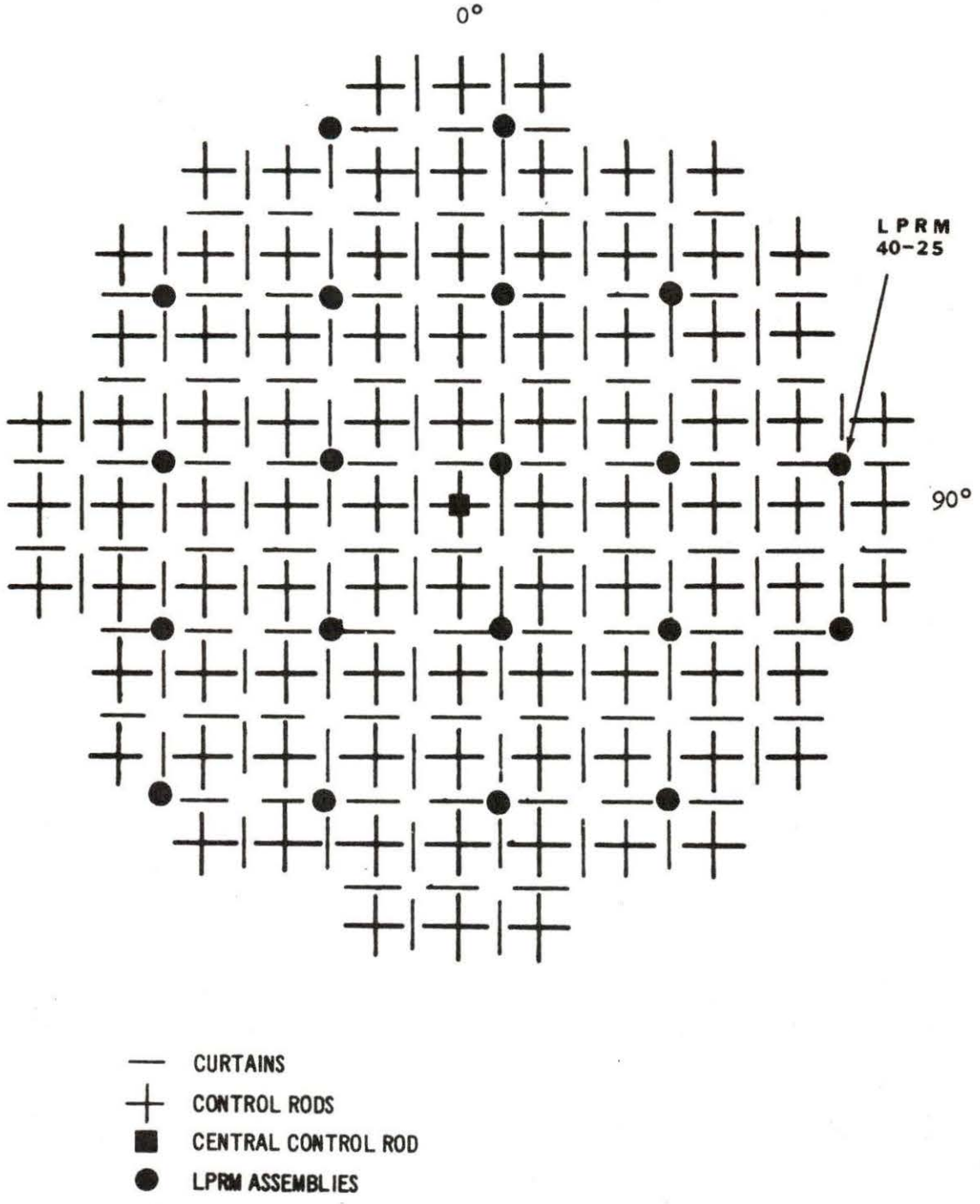

Fig. 2. Location of Local Power Range Monitor 40-25 in the DAEC core

1. Removal of the mean signal voltage, amplification of the analog noise data and recording of this data on magnetic tape at the reactor site.

2. Conversion of analog data to digital data and calculation of PSD's from digital data using FFT techniques and digital computers at an off-reactor site location.

Due to the amount of data needed for this study, the data acquisition equipment was left at the reactor site and operated by reactor engineering personnel. The data acquisition equipment consisted of a signal conditioning unit and an FM tape recorder. The tape recorder used was a Precision Instrument Company Model PI-6200 four channel FM tape recorder. The signal conditioning unit was a locally designed unit called SPARTAN (Signature Pattern Acquisition from ReacTor Amplified Noise). SPARTAN was designed and built to maximize the probability of correct acquisition of all data necessary to obtain a NPSD. SPARTAN allowed the mean signal to be biased out, this bias voltage to be measured, the noise signal to be amplified, the gain applied to the noise data to be logged, and the data recorded for the proper time interval.

To be analyzed, the recorded data were played back on the FM tape recorder and input to a device which filtered the data and converted the analog data to digital data. This filter/A-D device was designed and built by Harold Skank and his staff of the Ames Laboratory of DOE. The digital data were then input to the ALRR (Ames Laboratory Research Reactor) PDP-15 computer which calculated raw PSD's using a FFT program.

The FFT program was calibrated using a Hewlett-Packard Model 3722A Noise Generator.

C. Procedures

The noise signals were recorded three times a day in 20 minute data records. All four signals from the LPRM string were recorded in each data record. Nine data records were acquired during the week of October 10, 1977 and three data records were acquired on January 20, 1978. Only eight data records were acquired for detector A in October because of equipment failure. The reactor operating conditions for each data record are shown in Table 1.

Table 1. Reactor operating conditions for data acquisition

Tape Number	Date	Thermal power level (%)	Coolant flow rate (%)
23	10-10-77	100	100
24	10-12-77	100	100
25	10-13-77	100	100
27	1-20-78	90	100

The noise signals were then transported to the ALRR to be analyzed. These noise signals were then amplified and biased again to make the most efficient use of the A-D converter. The noise signals were then low passed filtered with an upper cutoff frequency of 10 Hz. To avoid aliasing (4), the sampling frequency (f_s) of the A-D converter should

be at least twice the highest frequency of interest. The f_s used was 25.6 Hz giving the highest usable frequency as 12.8 Hz. The FFT program used these digital points to calculate raw PSD's. To avoid side lobe leakage (4), the cosine square window function was applied to the entire data record. Two signals of each data record were analyzed at one time to allow computation of cross power spectral densities (CPSD), coherence, and phase lag of the two signals. For each combination of data signals, the raw PSD of each signal and the real and imaginary parts of the CPSD were calculated and stored on computer data cards. The real and imaginary parts of the CPSD were used to obtain the CPSD, coherence and phase (4).

Normalization of the raw PSD's was necessary to eliminate the dependence on reactor power level and to allow patterns from different reactors of similar design to be compared. This normalization of the raw PSD's creates NPSD (normalized power spectral density) and is very important. The idea of normalization was constantly used in all analysis and acquisition procedures and great care was taken to insure the normalization could be accomplished. The normalization factors used were:

1. A-D conversion
2. Filter gain
3. FFT calibration
4. $\overline{V}^2$, $\overline{V}$ = mean voltage of data signal
5. A_T^2, A_T = total amplification during data acquisition and pre-A-D conversion signal conditioning
6. Window function correction

7. $2/Nf_s$, this is a FFT factor (4).

The standard error ϵ of the PSD, after calculation, is given by (4)

$$\epsilon = \frac{1}{(B_e \cdot T_r)^{1/2}} \tag{5}$$

where B_e is the frequency resolution of the FFT and T_r is the finite time length of each data sample transformed. For the FFT, B_e is equal to $1/T_r$ therefore,

$$\epsilon = \frac{1}{(\frac{1}{T_r} \cdot T_r)^{1/2}} = 1.00 \tag{6}$$

This standard error is quite unacceptable. To decrease the standard error the FFT program averages 40 data samples which gives:

$$\epsilon = \frac{1}{(B_e \times 40 \times T_r)^{1/2}} = \frac{1}{(40)^{1/2}} \tag{7}$$

Frequency smoothing consists of combining neighboring frequency points and reduces the standard error and frequency resolution. Five point frequency smoothing was used because the resulting frequency resolution retained the characteristics of the original NPSD and enabled abnormal characteristics to be detected. In this case:

$$\epsilon = \frac{1}{(5 \times B_e \times 40 \times T_r)^{1/2}} = 0.0707 \tag{8}$$

Frequency smoothing was also carried out to increase the ease of handling the NPSD's in obtaining a signature pattern and subsequent malfunction detection. This statistical standard error (ϵ) is a theoretical lower limit on standard errors of further analysis processes and will only be used used when actual standard errors cannot be calculated. The standard

error calculated from noise data contains two error components. One component is the measurement standard error and the other is the reactor operating characteristics standard error.

V. EXPERIMENTAL RESULTS

A. Characteristics of Noise Signature Patterns

The comparison of NPSD's from one day to the next would not detect gradual changes in reactor operation and would provide useful information only if there were a sudden change in reactor operation. A more useful approach is the use of NSP's, noise signature patterns. Noise signature patterns for each distinct mode of operation, normal and abnormal, would be used to check for abnormal operating conditions. Use of noise signature patterns would facilitate the detection of gradual as well as sudden changes in reactor operational conditions. Since these noise signature patterns (NSP) are very important one must know how many normalized power spectral densities (NPSD) one needs to establish a NSP.

The data used to form Fig. 3 were obtained by averaging a successively larger number of NPSD's from October. This averaging procedure is demonstrated in Fig. 5. For each group of NPSD's averaged the composite standard error (CSE) was calculated using

$$CSE = \frac{1}{M} \sum_{k=1}^{M} \frac{\left(\frac{1}{N} \sum_{i=1}^{N} (NPSD_{ik} - Z_k)^2\right)^{1/2}}{Z_k} \qquad (9)$$

where M is the number of frequency points used in the NPSD, N is the number of NPSD's averaged, $NPSD_{ik}$ is the ith NPSD point at the kth frequency point and Z_k is the kth frequency point of the averaged NPSD. The composite standard error (CSE) is a measure of the range of variation for the NPSD's averaged. If the NPSD's averaged were very similar, shown in Fig. 5, the CSE would be small. If the NPSD's averaged were

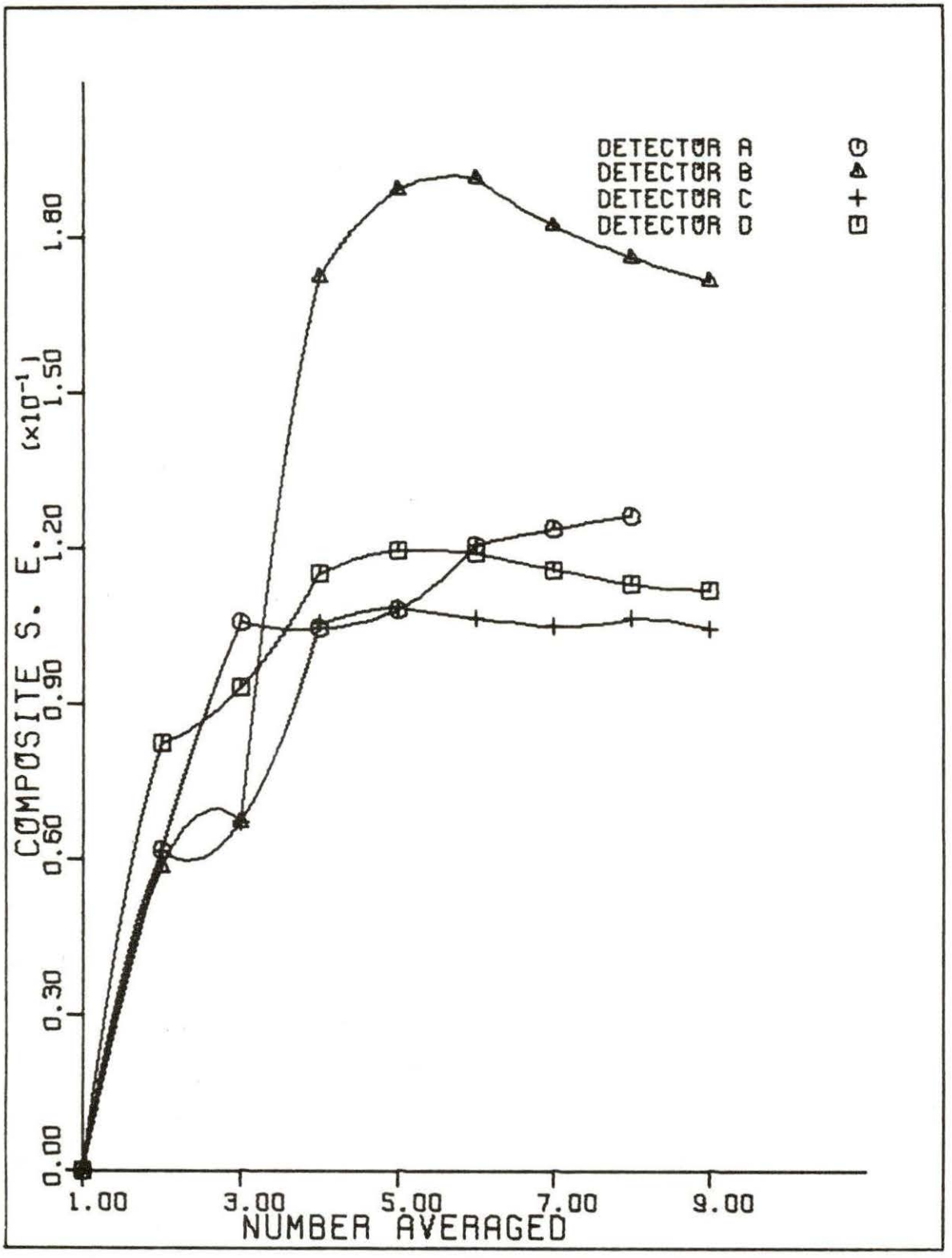

Fig. 3. Composite standard error as a function of the number of NPSD's averaged

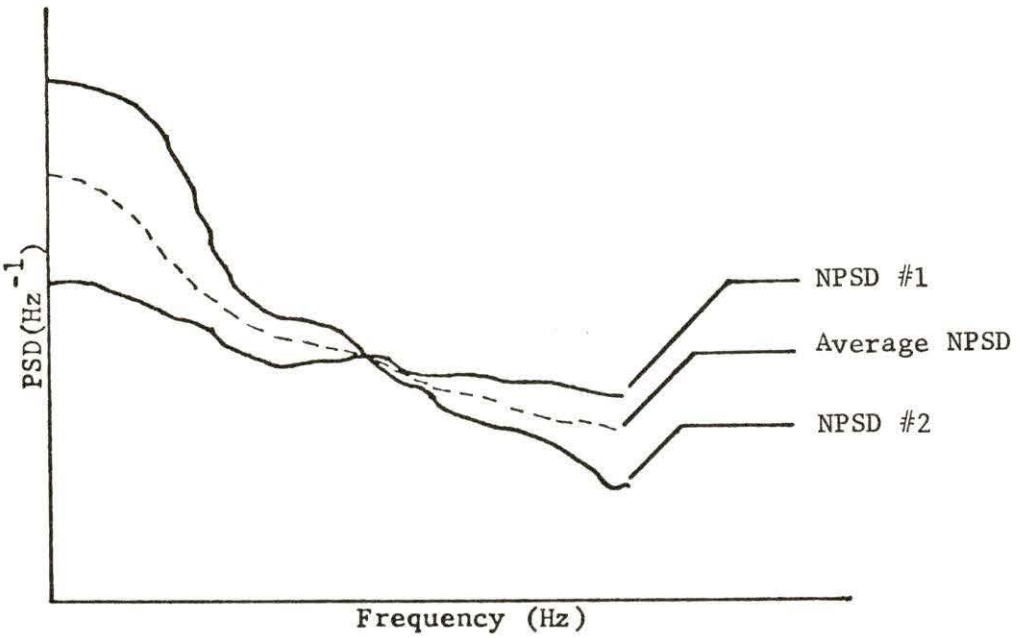

Fig. 4. Averaging two unsimilar NPSD's

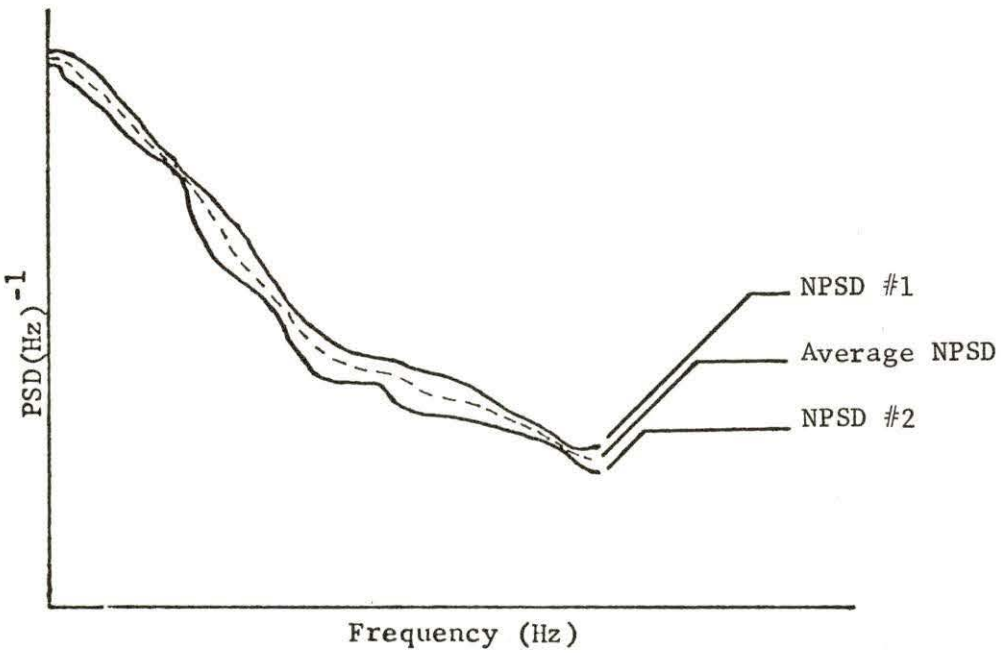

Fig. 5. Averaging two similar NPSD's

not so similar, shown in Fig. 4, the CSE would be large. Figure 3 gives an indication of how many NPSD's are needed to obtain a noise signature pattern (NSP). The CSE increases as the number of NPSD's averaged increases until at six NPSD's the CSE becomes approximately constant. This constant CSE indicates that the range of variation for the NPSD's has been defined. Once this range of variation has been defined, the average NPSD of this group of NPSD's can be classified as a noise signature pattern. Thus, the NSP for this set of reactor conditions and detectors has been established for the data acquired in October. The January data set cannot be used to form a NSP since it contains only half of the six data records necessary.

The amount of data needed for a NSP is an important question to have answered. Another important question to be answered is, what is the length of time a NSP is valid if reactor operating conditions are kept constant? Of course, time is also an operating condition since the core's composition and configuration will change with time because of fuel burn-up and normal wear, respectively. The length of time a NSP is valid can be partially determined by comparing the October data set to the January data set. The CSE's for all the data records from October are 0.126, 0.172, 0.104, and 0.112 for detector A, B, C, and D respectively. When the January data records are combined with the October data records the CSE's are 0.254, 0.169, 0.114, and 0.137 for detector A, B, C, and D respectively. This change in the CSE's indicates that the NSP's obtained from October data are valid for a period of time less than three months.

The data from October can be used to form NSP's, and these are shown in Figs. 6-9. These NSP's are very similar in shape and magnitude to NPSD's obtained by Fry et al. (9). The 0-2 Hz range is governed by the large global effects, and the 2-10 Hz range by the local noise sources.

Normalized root-mean-square (NRMS) values are proportional to the area under a NPSD curve. NRMS values for several frequency ranges for the four NSP's are given in Table 2. The interesting point of this table is the NRMS levels for the NSP's in 2-9.4 Hz range. This is the range where local noise sources are dominant. The NRMS values, in the 2-9.4 Hz range, indicate that detector A has the largest amount of neutron noise followed by C, B, and lastly D with the least amount of noise. In normal reactor operation, with no abnormal vibration, coolant void formation is the major noise source in the 2-10 Hz range. Thus, one would think that detectors A and D should have their positions reversed in the order of noise level. The D, C, B, A order of neutron noise levels in the 4-10 Hz range was reported by Blomberg and Akerhielm (5) for the 440 MW Oskarshamn I BWR. Ando et al. (2) also reported the D, C, B, A order of noise level in the 1-10 Hz range for the 460 MW Fukushima I BWR. The Oskarshamn and Fukushima reactors have core configurations that are different from the DAEC, so no conclusions can be drawn until more is known about correlating noise data from reactors with different core configurations.

Holthaus (13) reported a decrease of the negative slope of NPSD's in the 1-10 Hz range as detector height in the core increases. The NSP's obtained in this study exhibit that same trend from 2-9.4 Hz.

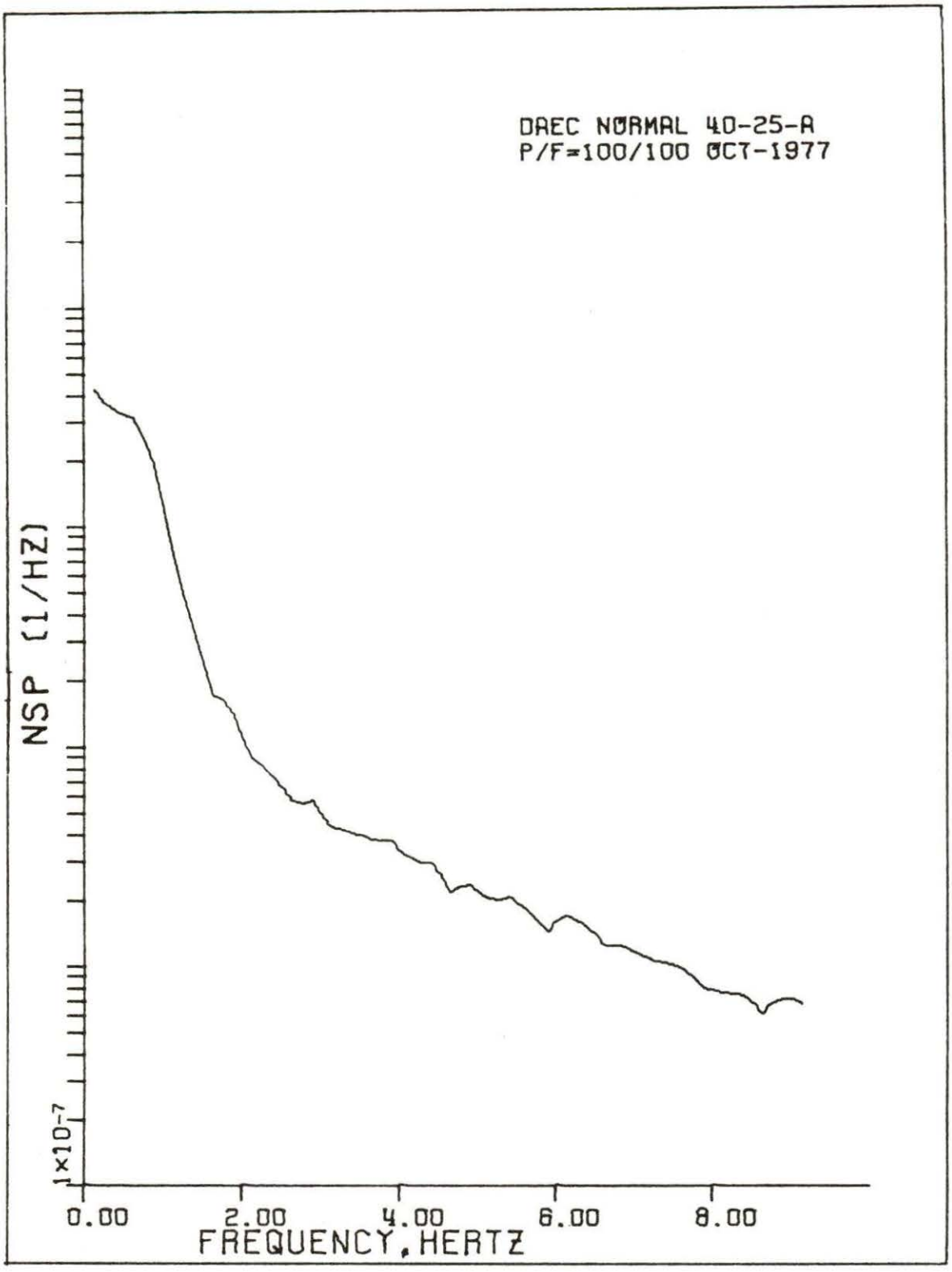

Fig. 6. Noise signature pattern for detector A in October

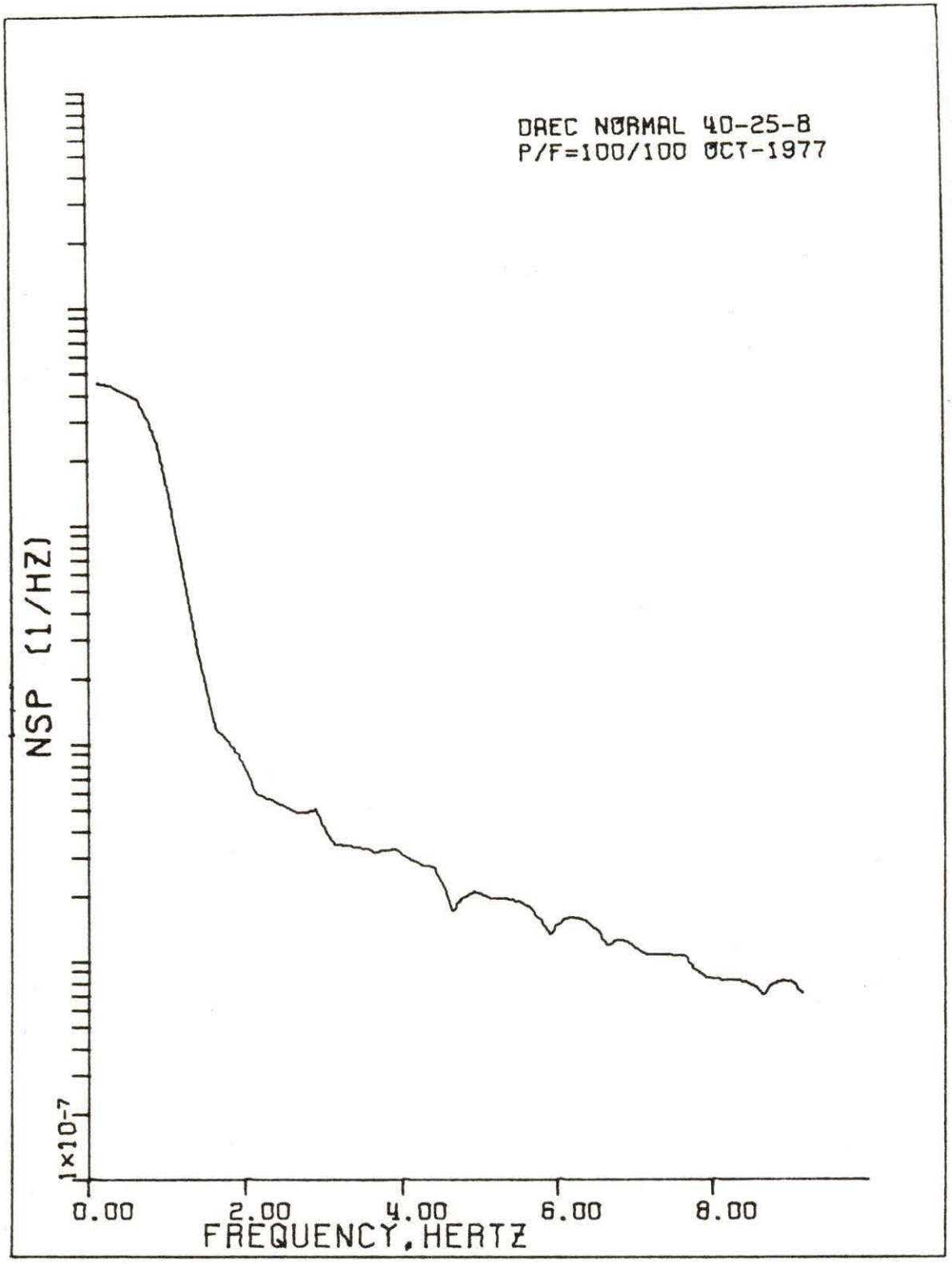

Fig. 7. Noise signature pattern for detector B in October

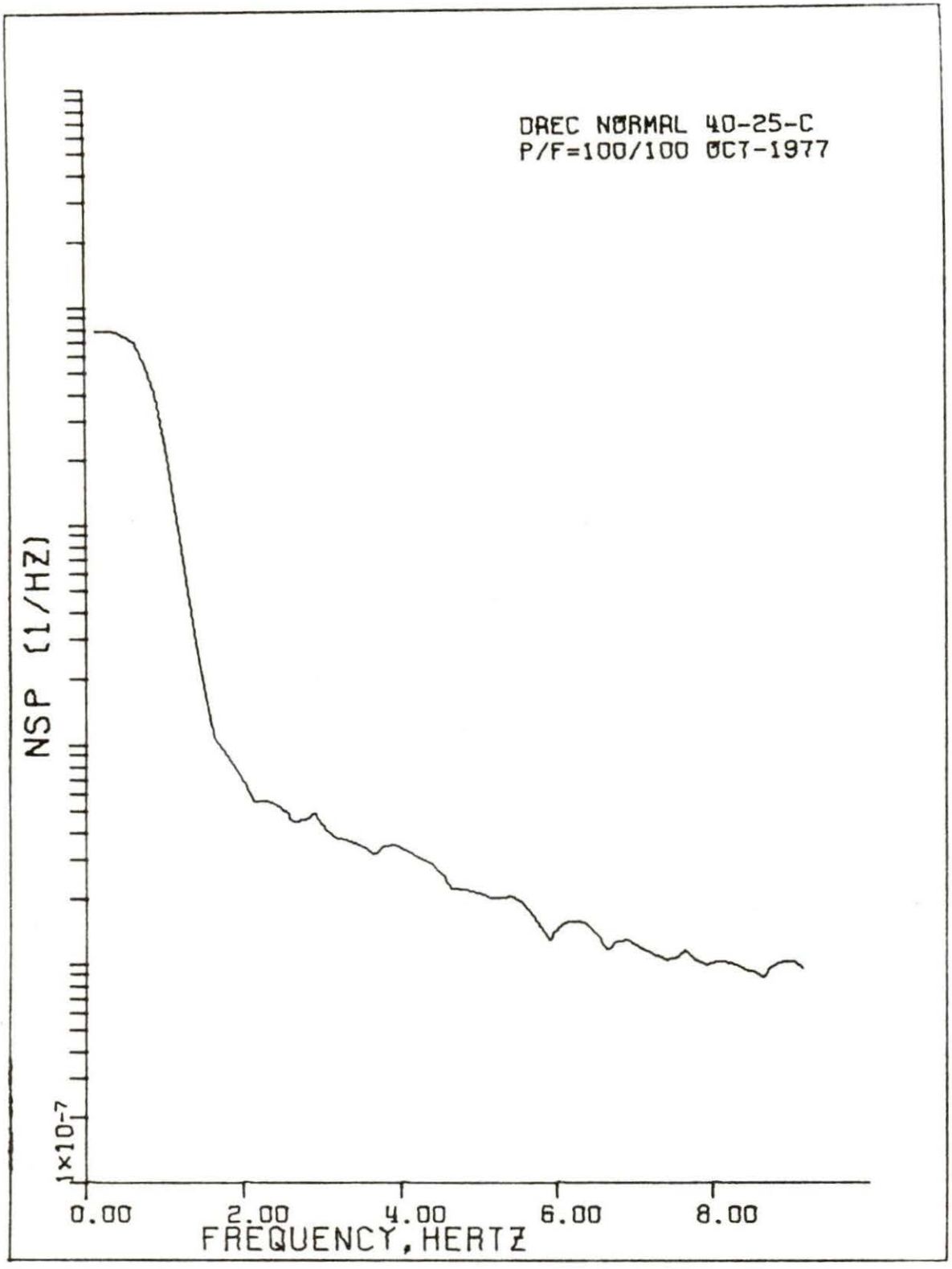

Fig. 8. Noise signature pattern for detector C in October

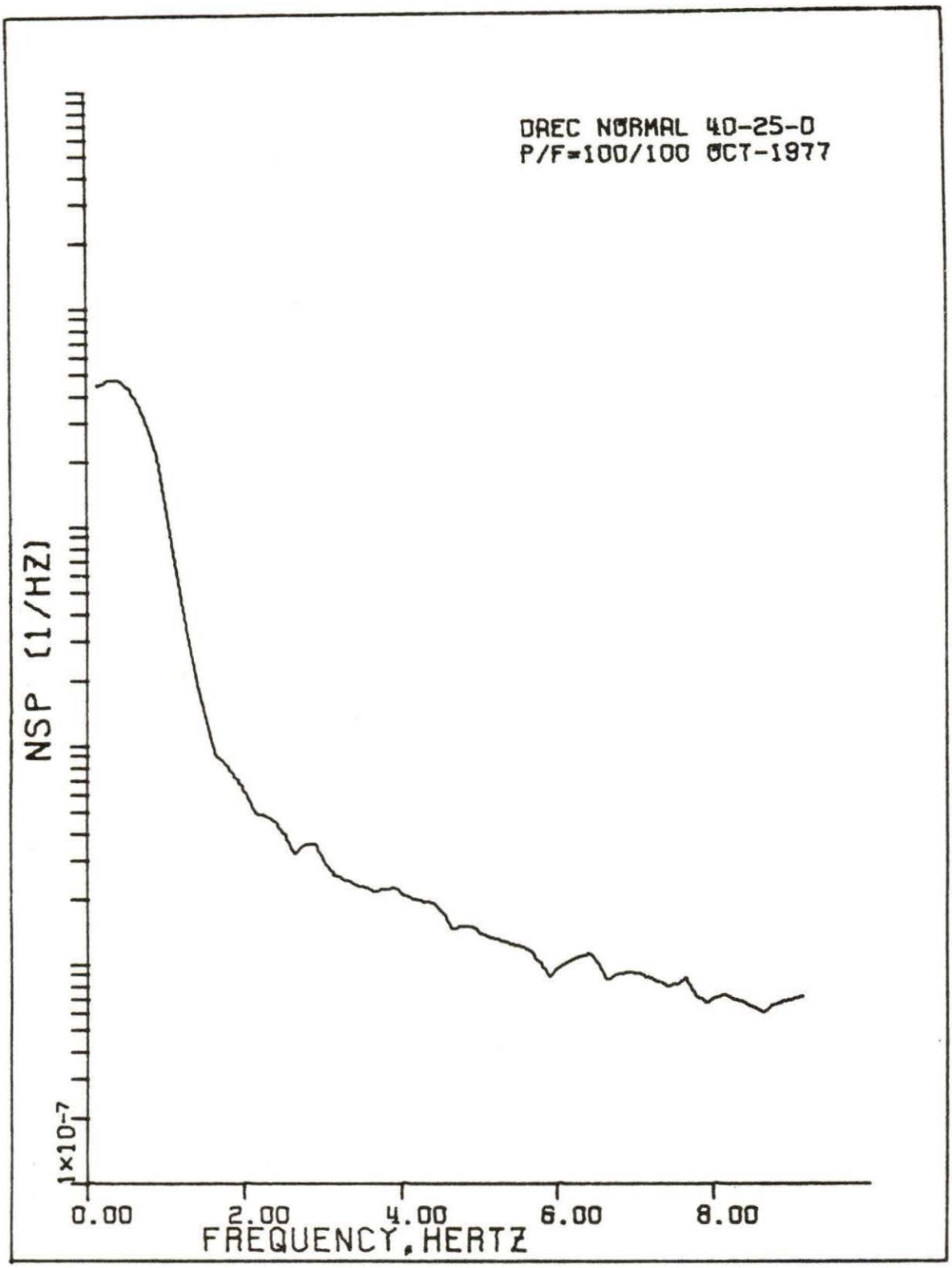

Fig. 9. Noise signature pattern for detector D in October

Table 2. Normalized RMS values for the NSP's

NSP	NRMS 0.05-9.4 Hz range	NRMS 0.05-2 Hz range	NRMS 2-9.4 Hz range
40-25-A	$1.78(10^{-2})$	$1.36(10^{-2})$	$4.20(10^{-3})$
40-25-B	$1.91(10^{-2})$	$1.52(10^{-2})$	$3.93(10^{-3})$
40-25-C	$2.48(10^{-2})$	$2.08(10^{-2})$	$4.00(10^{-3})$
40-25-D	$1.89(10^{-2})$	$1.55(10^{-2})$	$3.37(10^{-3})$

Detector A has a slope of $-8.95(10^{-7})$, detector B has a slope of $-7.42(10^{-7})$, detector C has a slope of $-6.91(10^{-7})$, and detector D has a slope of $-5.09(10^{-7})$. The units of these slopes are $(1/Hz^2)$. The slopes were calculated using points (2.9 and 8.65 Hz) that were a good indication of the pseudolinear portion of the pattern.

Normalized cross power spectral densities (NCPSD) can provide information because noise sources common to two detectors can be detected. Severe vibration or impacting of objects in the core would cause noise common to more than one detector and this vibration or impacting would cause an increase in the NCPSD at the frequency of the vibration. Coherence is another important function to consider in combination with NCPSD's. The NCPSD's obtained from DAEC detectors C and D are similar to those obtained by Mathis et al. (16), in shape and magnitude. The coherence function generated from DAEC noise data for C and D is similar in shape to that obtained by Mathis et al. (16), but the DAEC coherence is 50% less than Mathis' coherence for the 1-5 Hz range and approximately equal for the 5-9.4 Hz range. Mott et al. (18) has set forth specific

criteria for the detection of LPRM instrument tube impacting against fuel boxes in BWR-4's. These criteria are:

1. NCPSD $> 2(10^{-6})$ in the 4 Hz region and
2. Coherence > 0.2 in the 4 Hz region

and should be applied to the top two detectors in the detector string, C and D. All the NCPSD's obtained from DAEC for C and D detectors were less than $2(10^{-6})$ and had corresponding coherence values of less than 0.2 for the 4 Hz region. In March, following the noise data acquisition, DAEC went through refueling procedures. The 40-25 LPRM detector was visually inspected for excessive wear. No excessive wear or evidence of impacting was found.

Coherence and NCPSD functions indicate the break point in frequency between global and local neutron noise sources. Global noise sources affect the entire core and all detectors would have high coherence and NCPSD values in the frequency range of the global noise. Figures 10-13 and 14-17 are of representative NCPSD and coherence functions and indicate the frequency break point for global and local noise sources is approximately 2 Hz. This result agrees with Fry et al. (9).

Phase lag data can give the coolant void velocity between two detectors. Void velocities (V_v) can be calculated using

$$V_v = \frac{L}{\tau} \tag{6}$$

where L is the distance between the two detectors, and τ is the slope of the phase versus frequency, shown in Figs. 18-20. τ is in Deg/Hz and must be multiplied by 1/360 to be converted to seconds. The calculated V_v from B to C is 18.1 ft/sec and is 21.7 ft/sec from

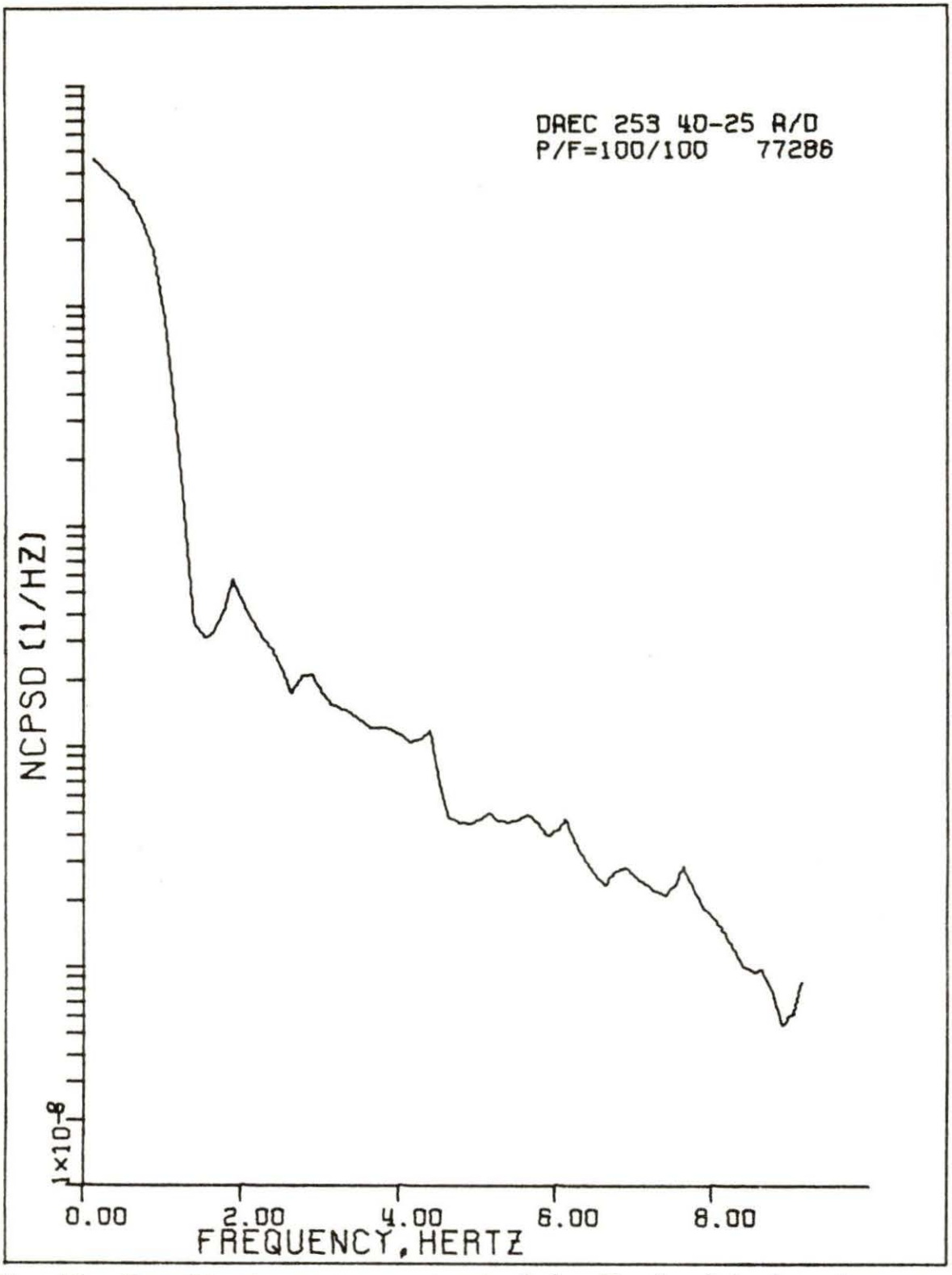

Fig. 10. Normalized cross power spectral density for detectors A and D in October

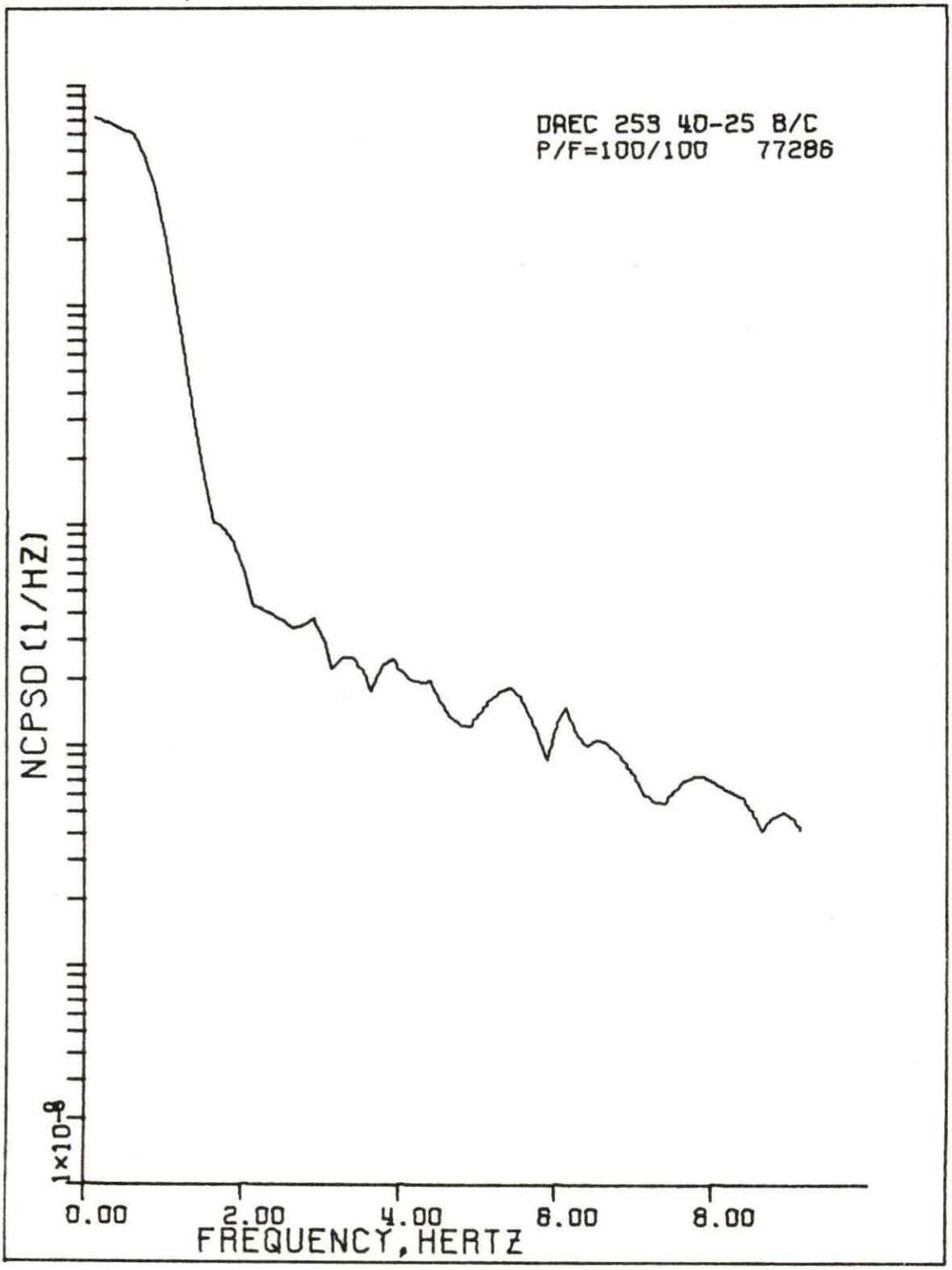

Fig. 11. Normalized cross power spectral density for detectors B and C in October

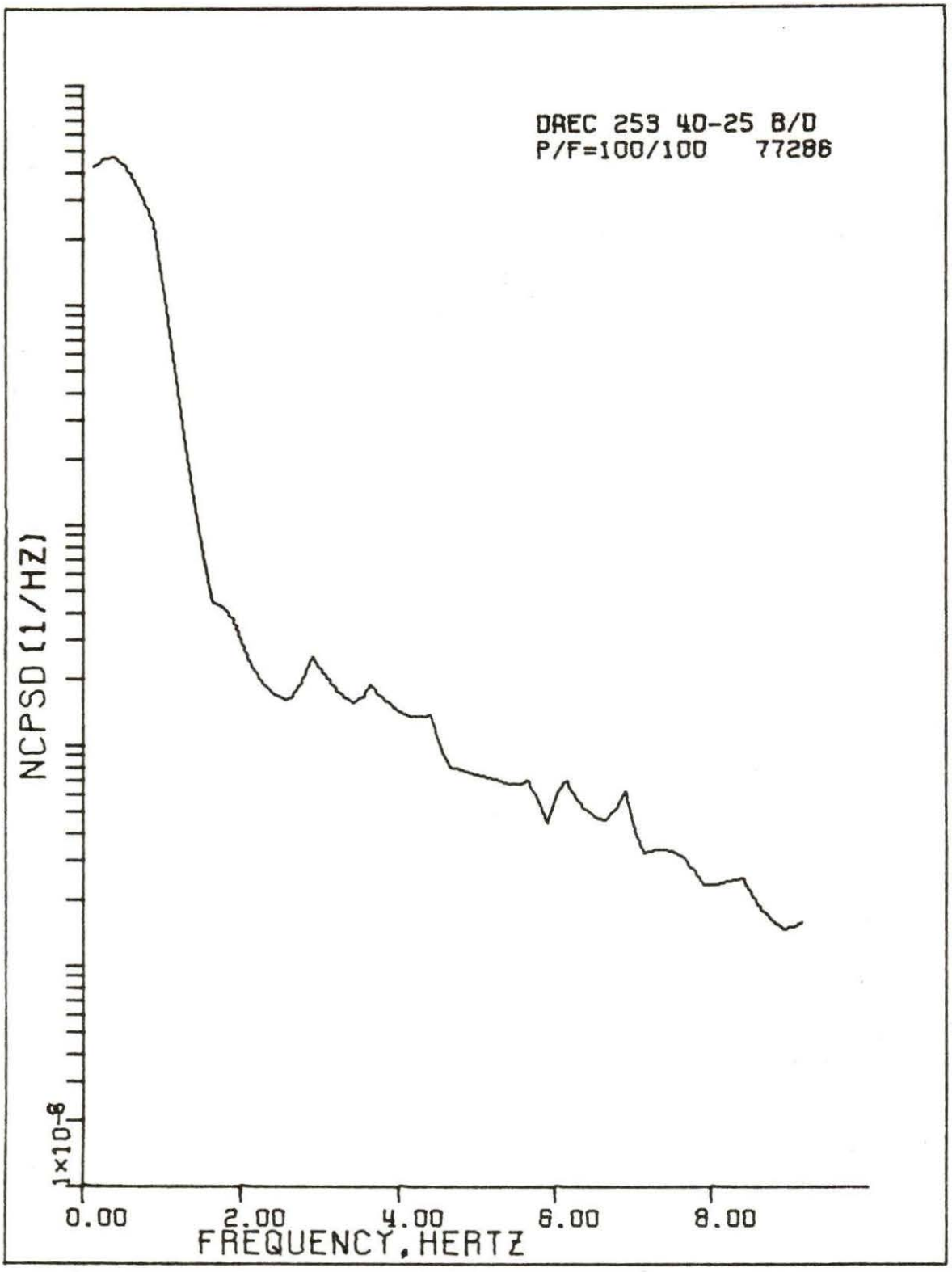

Fig. 12. Normalized cross power spectral density for detectors B and D in October

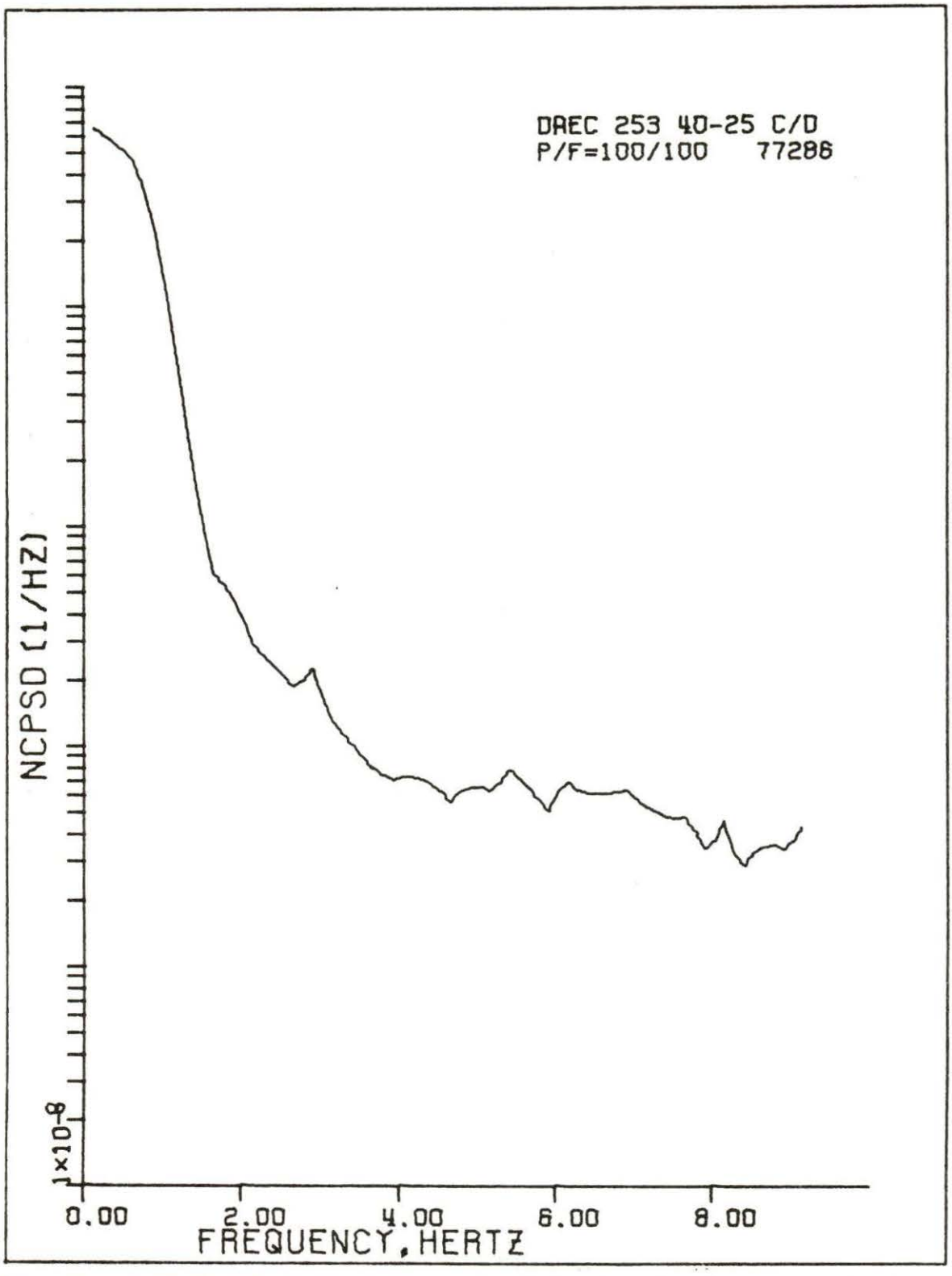

Fig. 13. Normalized cross power spectral density for detectors C and D in October

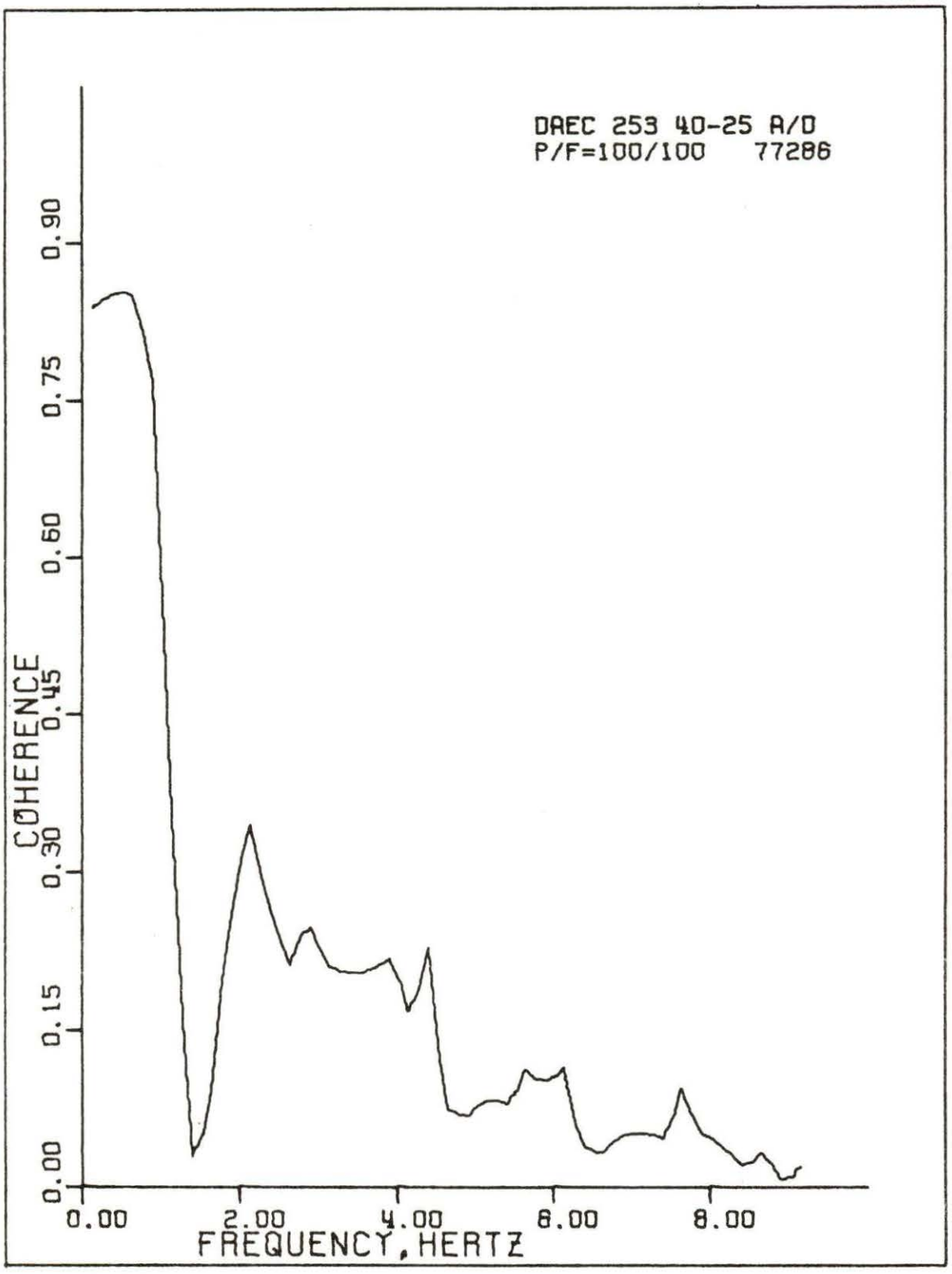

Fig. 14. Coherence between detectors A and D in October

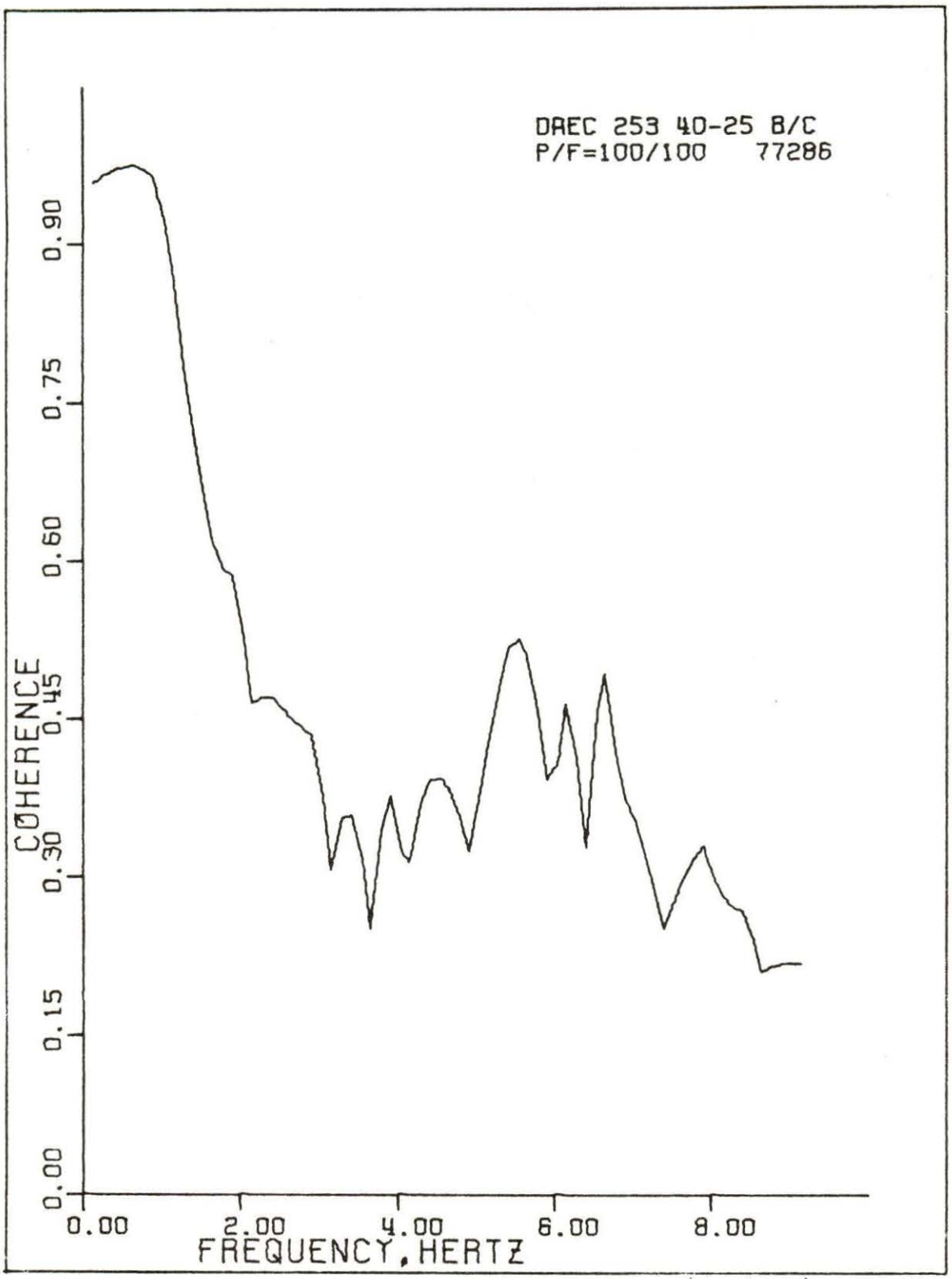

Fig. 15. Coherence between detectors B and C in October

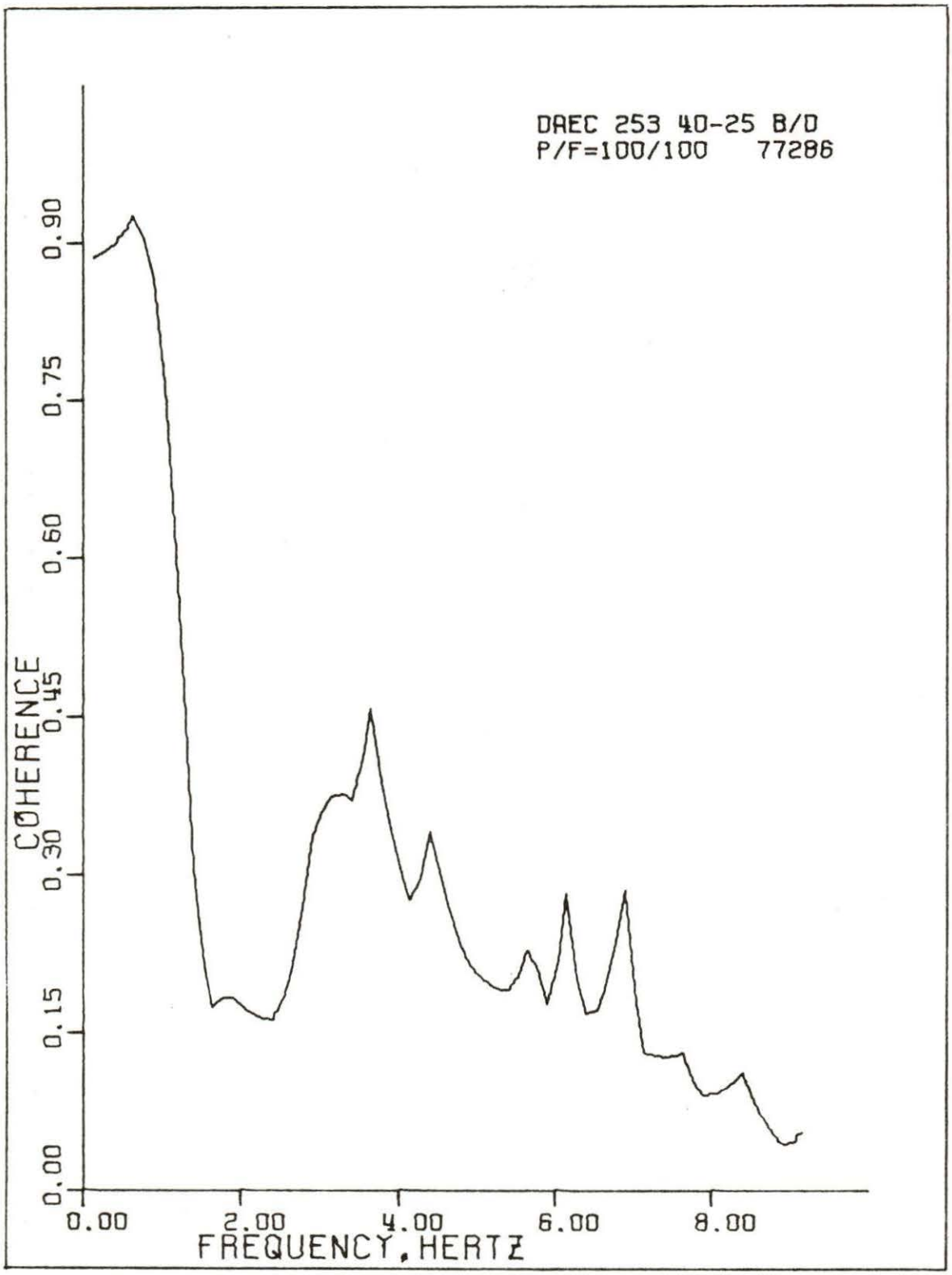

Fig. 16. Coherence between detectors B and D in October

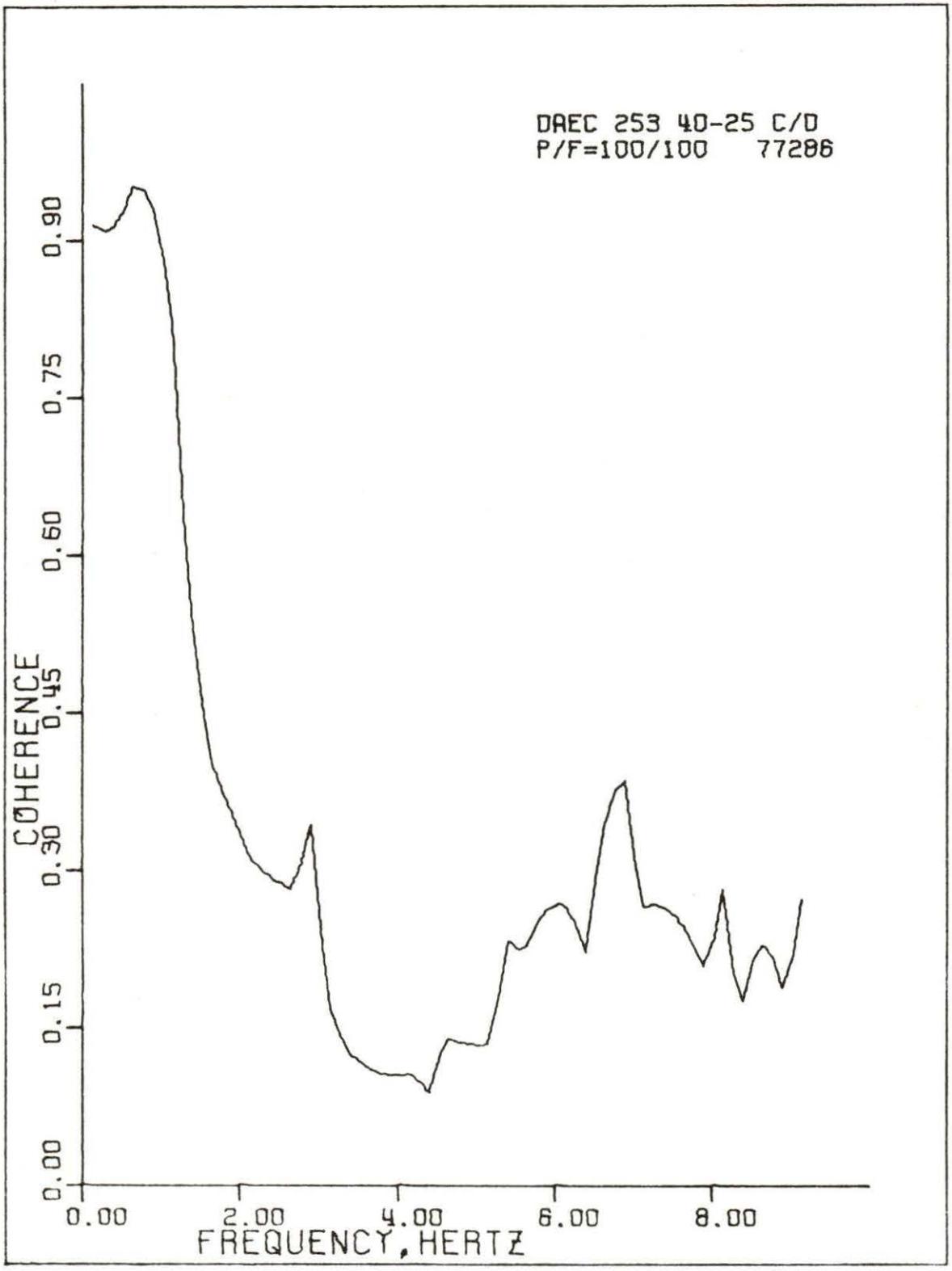

Fig. 17. Coherence between detectors C and D in October

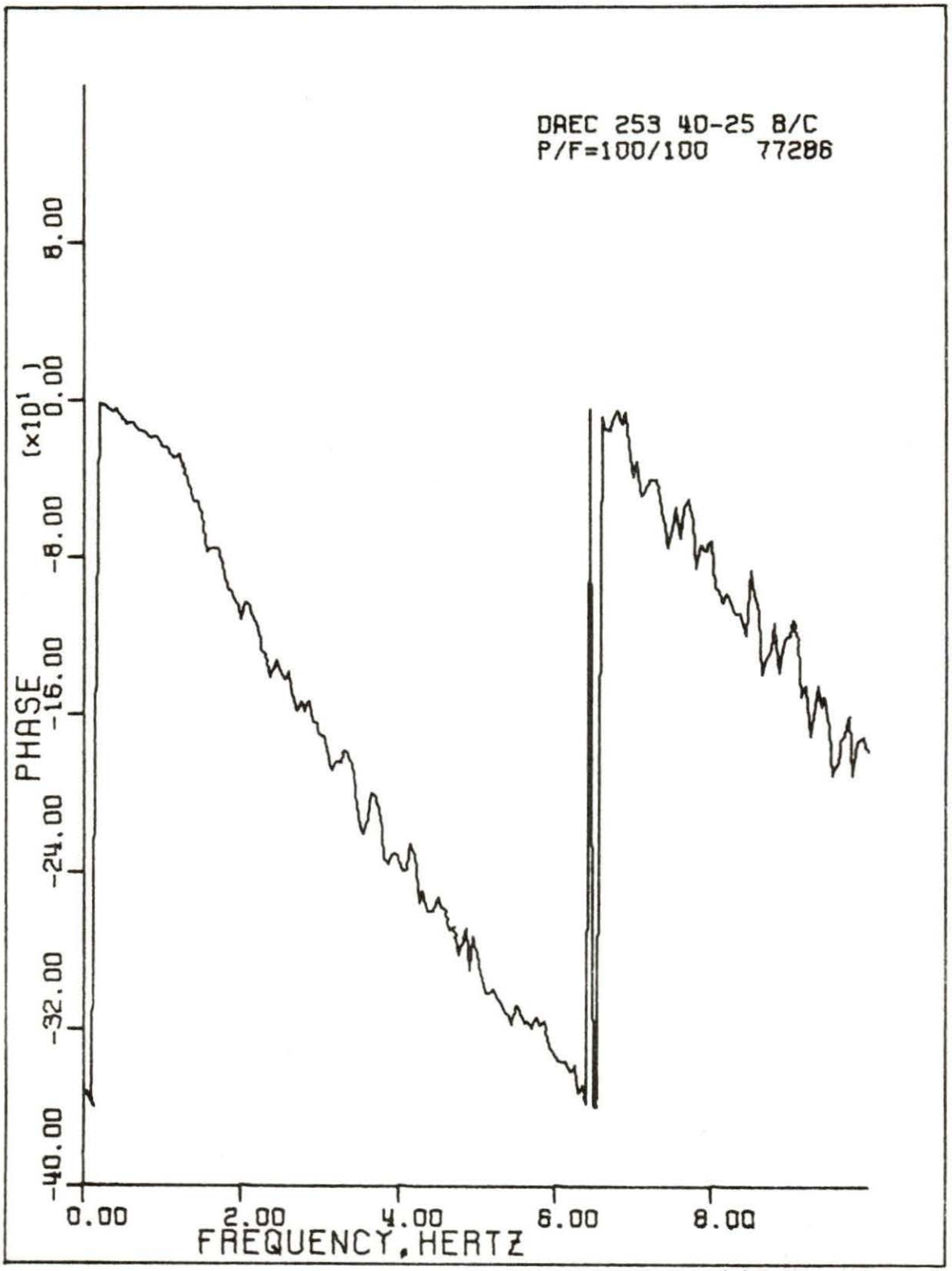

Fig. 18. Phase lag between detectors B and C in October

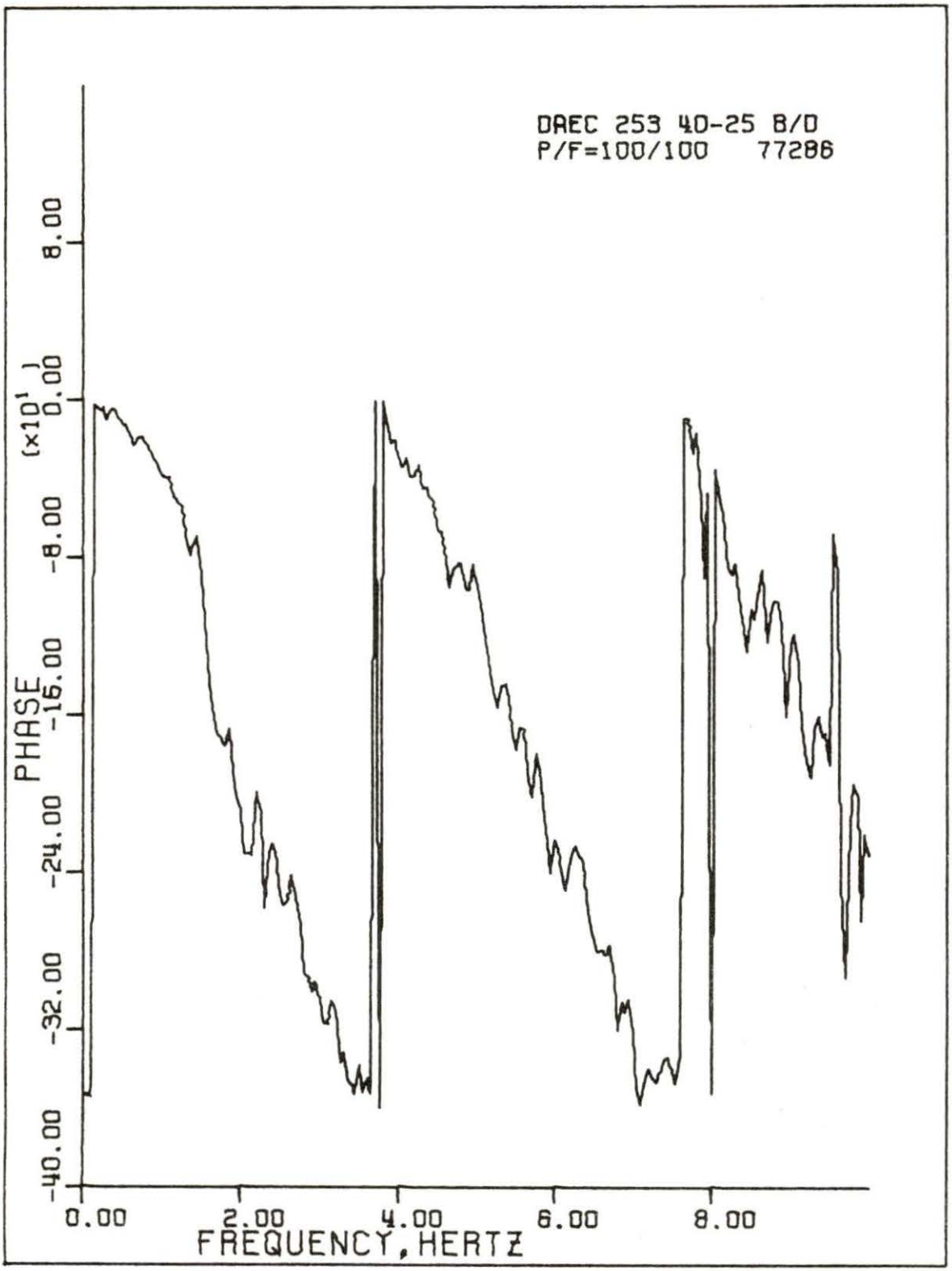

Fig. 19. Phase lag between detectors B and D in October

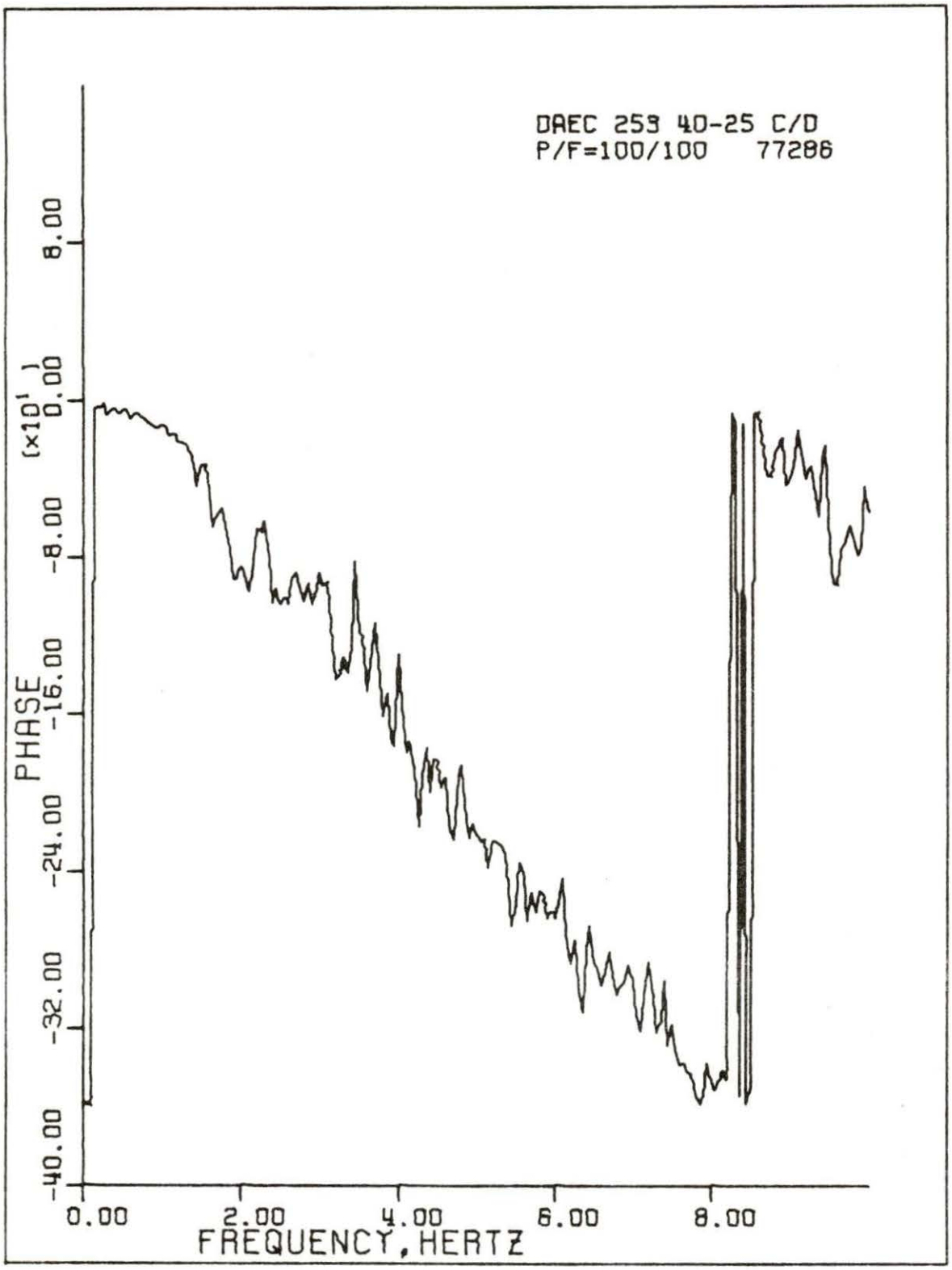

Fig. 20. Phase lag between detectors C and D in October

C to D. These velocities agree well with velocities calculated from the Hatch-1 BWR by Atta et al. (3).

B. Application to Reactor Monitoring

Neutron noise analysis can be useful to reactor monitoring if used with a complete library of NSP's for normal and abnormal reactor conditions. NSP's can be used in two ways. The first way is in the form of a characteristic NRMS value and the second way is a NSP covering the frequency range of interest.

Neutron noise is a statistical process. Therefore, the NSP and NRMS values obtained from this noise are statistical in nature and have statistical errors associated with them. This statistical error can be interpreted as the allowable variation of the value under study. Two such statistical values are said to be equal if they are in the range of each other's statistical error. The statistical error, or allowable variation, is impossible to calculate theoretically for power reactor noise. Therefore, the variation of the data must be used to establish the allowable variations of the data.

The allowable variation in the NRMS values was found by noting the variation in the NRMS values of the NPSD's used to form the signature patterns for October; these results are given in Table 3. Any NRMS value for any detector outside the limits given in Table 3 would be a prime object for further analysis. The allowable variation in the NSP for any one frequency point was determined by noting the maximum fractional deviation for any one frequency point of all the NPSD's

Table 3. Allowable variations for NRMS values and NSP fractional deviations to be used in the monitoring system

NSP	NRMS 0.05-9.4 Hz	NRMS 2-9.4 Hz	Maximum fractional deviations
A	$1.72(10^{-2})$ to $1.85(10^{-2})$	$3.96(10^{-3})$ to $4.48(10^{-3})$	0.51
B	$1.64(10^{-2})$ to $2.07(10^{-2})$	$3.43(10^{-3})$ to $4.27(10^{-3})$	0.41
C	$2.30(10^{-2})$ to $2.79(10^{-2})$	$3.75(10^{-3})$ to $4.42(10^{-3})$	0.39
D	$1.84(10^{-2})$ to $1.96(10^{-2})$	$3.22(10^{-3})$ to $3.69(10^{-3})$	0.53

used to form the signature pattern. These fractional deviations were calculated using

$$FD_k = \frac{|NPSD_k - NSP_k|}{NSP_k}$$

where k refers to the frequency point. These maximum fractional deviations are given in Table 3. If, in comparing a NPSD to a signature pattern, any frequency of the NPSD has a fractional deviation greater than the maximum fractional deviation for that detector then that frequency of the NPSD is in question.

NSP's could be used in three stages:

1. NRMS values are calculated daily and if trouble is indicated, stage 2 is used.

2. The NPSD is calculated and compared to the NSP over a few frequency ranges known to indicate abnormal reactor conditions.

3. The present NPSD is compared to the NSP over the entire frequency range.

The NRMS calculation is convenient and inexpensive because it requires none of the complicated computer programming necessary for a NPSD calculation. The procedure for NRMS monitoring would be:

1. Sample detector signal in question to establish the mean value $\overline{V}$ of the signal.

2. Low pass filter the signal with the upper cutoff frequency of 10 Hz.

3. Digitize the analog signal at no less than 20 samples per second.

4. Subtract $\overline{V}$ from all digitized points.

5. Square and average all digitized points.

6. Find the square root of the value calculated in #5.

7. Compare NRMS value from step #6 to allowable range of NRMS values.

The second stage of monitoring would be in the frequency domain and would be composed of a quick comparison, on a fractional deviation basis, of the present NPSD to the NSP at a few frequency ranges known to contain trouble areas. The frequency range of 0-2 Hz and 8-10 Hz have not been shown to contain information about abnormal vibrations. Therefore, these frequency ranges could either be ignored or be reduced to one datum point for each range. It has been indicated by Mott et al. (18) and Holthaus (13) that the 2-8 Hz frequency range contains a large

portion of the vibrational information. Mathis et al. (17) and Holthaus (13) have shown that abnormal peaks in the 2-8 Hz range are usually 1-2 Hz wide at their maximum width. Therefore, frequency resolution of 0.5 Hz would insure detection of an abnormal signal. The second stage of analysis would be comprised of comparisons of the present NPSD to the normal NSP with one frequency point in each of the 0-2 Hz and 8-10 Hz ranges and frequency points at 0.5 Hz interval in the 2-8 Hz range.

The third stage of analysis would be either a total NPSD-to-NSP comparison or a segment of the NPSD compared to the NSP. If the frequency range of the abnormal signal was detected in step 2 then that frequency range would be examined using the highest frequency resolution possible. This abnormal signal could then be compared with other well-defined abnormal signals. If the frequency range of the abnormal signal was not detected by step 2 then a full NPSD, at moderate frequency resolution, could be compared to the NSP to detect the abnormal signal. Once detected, the abnormal signal's frequency range could be closely examined.

To check the monitoring system an abnormal NPSD was analyzed. The abnormal NPSD was generated by superimposing a segment of an abnormal PSD upon a NPSD for detector D, shown in Fig. 21. The abnormal PSD was obtained by Holthaus (13) in June of 1975 when the DAEC was experiencing LPRM tube vibrations and impacting against channel boxes. The data of Holthaus were not normalized so only PSD's (power spectral densities) were produced, shown in Fig. 22. The portion of the PSD that is abnormal is the peak in the 3-5 Hz range. Because the abnormal data were not normalized the abnormal peak could not be directly

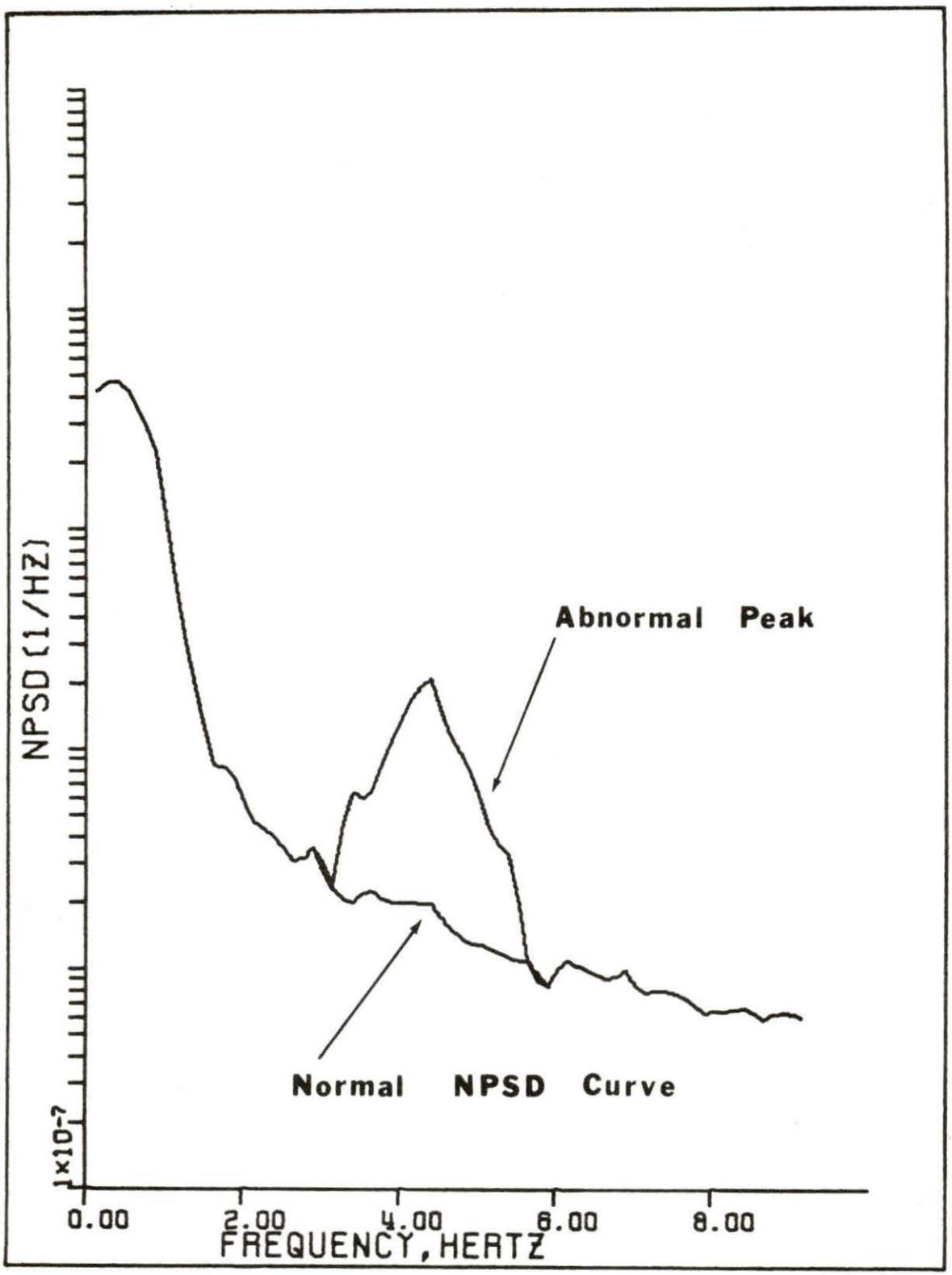

Fig. 21. Abnormal peak used in testing monitoring criteria

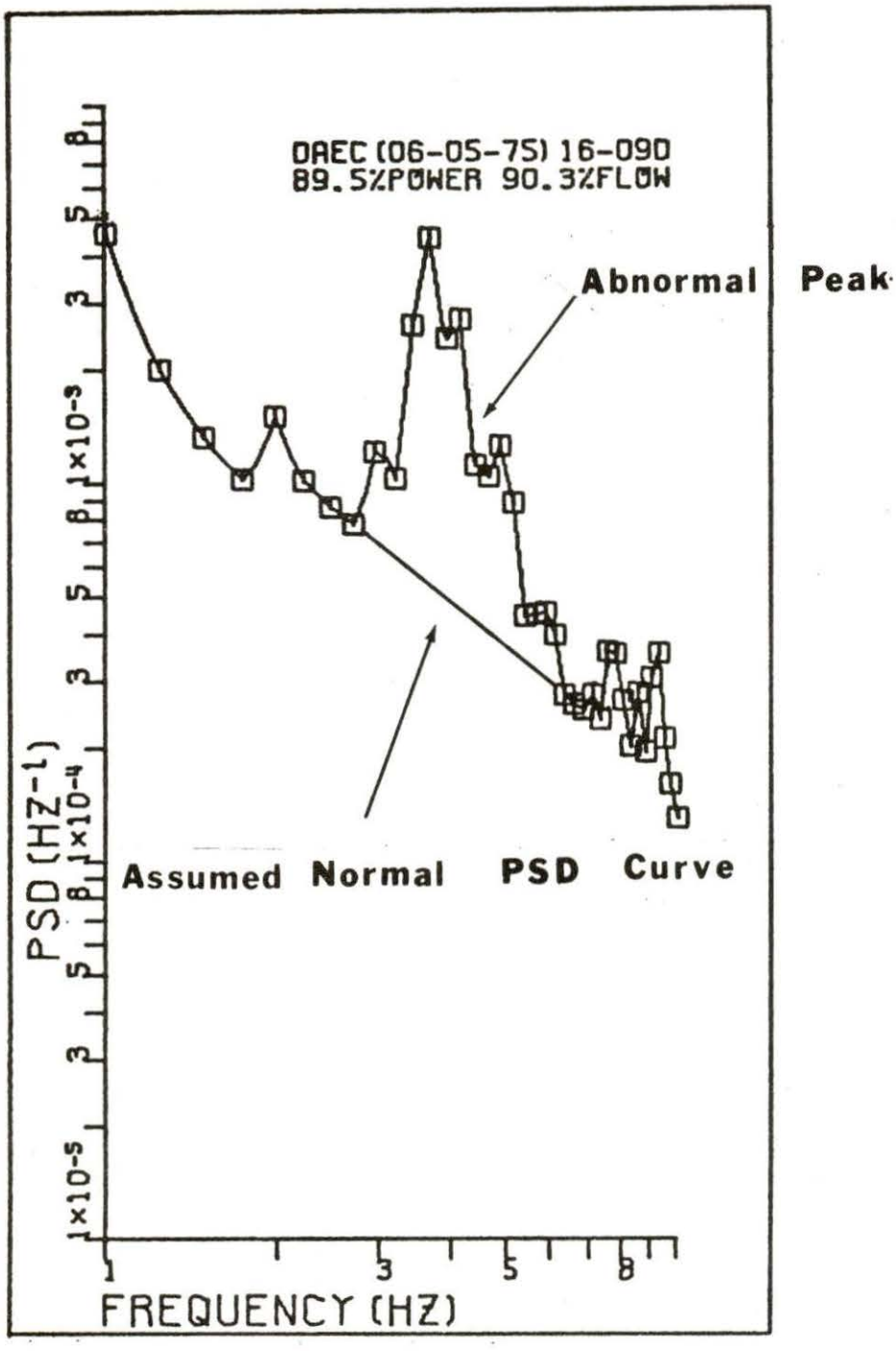

Fig. 22. Noise signature for the 16-09D LPRM (June 5, 1975)

superimposed upon the present NPSD. The percentage increase of the abnormal peak to the assumed normal PSD curve for Fig. 22 was calculated. These percentage increases were then applied to the NPSD curve of Fig. 21 to produce the abnormal peak of Fig. 21.

Four different abnormal peaks were generated to test the sensitivity of the monitoring system. These abnormal peaks are as follows:

1. Total abnormal peak area
2. 0.4 abnormal peak area
3. 0.2 abnormal peak area
4. 0.08 abnormal peak area.

The results of the analysis of the abnormal peaks using the monitoring system are shown in Table 4.

Comparison of NRMS in the 0.05-9.4 Hz range to the allowable NRMS values shown in Table 3 indicate no abnormal signal but, comparison in 2-9.4 Hz range indicates an abnormal signal in three of the four cases. The fourth signal would represent a small departure from normal conditions and most likely no damage would be done by this small deviation from the normal. The large noise levels of the global effects mask the variation in the 2-9.4 Hz noise levels. Therefore, in using NRMS values as an indication of abnormal conditions only the 2-9.4 Hz range should be used. The 2-8 Hz range could also be used since this range contains a large portion of the vibrational information.

Comparison of allowable fractional deviations to the abnormal fractional deviations indicated abnormal conditions in all four signals. This result supports the use of fractional deviation comparison as the more detailed method for the monitoring of reactor conditions because of its sensitivity.

Table 4. Abnormal NPSD data for detector D

Signal	NRMS 0.05-9.4 Hz	NRMS 2-9.4 Hz	Fractional deviation with respect to the NSP for detector D
Total abnormal peak	$1.90(10^{-2})$	$5.41(10^{-3})$	9.99
0.4 abnormal peak	$1.88(10^{-2})$	$4.25(10^{-3})$	8.79
0.2 abnormal peak	$1.87(10^{-2})$	$3.77(10^{-3})$	1.99
0.08 abnormal peak	$1.86(10^{-2})$	$3.46(10^{-3})$	1.67

The ideal method of reactor monitoring using noise analysis is dependent on a complete library of noise signature patterns for every phase of normal reactor conditions and any possible abnormal conditions. Also, the suggested monitoring system is just that, a suggestion. It is based on the limited amount of information available and should not be taken as all inclusive and functional. Instead, it is only a place to start to develop more sophisticated methods.

VI. CONCLUSIONS

The equipment and procedures developed by this study permit the relatively easy and low cost acquisition of noise data. These two improvements were provided by the data acquisition equipment's ability to be left at the reactor site. The data are then acquired by reactor engineering personnel with little or no interruption to their normal activities. The researcher can set up the data acquisition equipment and not return to the reactor site until the desired amount of data have been acquired. It is possible to leave the equipment at the reactor site for days or even weeks to acquire data and be assured all necessary data have been recorded. Researchers and reactor personnel must work together to acquire the large amount of baseline data necessary to achieve confidence in neutron noise analysis.

The amount of data, i.e., NPSD's, needed to establish a noise signature pattern was determined. Six to nine NPSD's need to be averaged to produce a signature pattern. This result is supported by the composite standard error "plateau" formed in Fig. 3.

The time interval a NSP is valid was determined as less than three months. The CSE for detector A using October data is 0.126. When the January data was combined with the October data, the CSE for detector A increased 101.5%. Similar changes in the CSE of 1.5%, 9.6%, and 22.7% were observed for detector B, C, and D respectively. These changes in the CSE's indicate a change in NPSD's from October to January.

NSP's have decreasing negative slopes, in 2-9.4 Hz range, as detector height in the core increases. The slope becomes less negative

because of an increase in noise in the high (10 Hz) frequency range. The increase in noise is due to increased coolant void formation.

Detector C displayed the largest amount of global noise followed by D, B, and A. Detector A displayed the largest amount of local noise followed by C, B, and D. These conclusions are supported by the results in Table 2.

Coherence and NCPSD functions indicate that the frequency range of 0.05-9.4 Hz is composed of two regions with different characteristics. The first region is from 0.05 Hz to approximately 2 Hz. In this region the coherence and NCPSD functions have initially high values which decrease rapidly as frequency increases. In the second region, 2-9.4 Hz, the NCPSD function decreases with a constant slope. The 2-9.4 Hz region of the coherence function has much lower values and fluctuates more rapidly than the 0.05-2 Hz region. The 0.05-2 Hz region is dominated by global noise effects and the 2-9.4 Hz region is dominated by local noise effects.

Phase lag functions can be used to calculate coolant void velocities. Void velocities obtained in this study agree with velocities calculated by Atta et al. (3).

A reactor monitoring procedure utilizing neutron noise analysis was successfully tested using actual abnormal neutron noise data. The monitoring procedure consists of three stages, each stage progressively more expensive in time and money and providing more precise information. NRMS analysis detected an abnormal signal five times smaller than the actual abnormal noise signal for LPRM instrument tubes impacting against channel boxes. The comparison of NPSD's to signature patterns, on a fractional deviation basis, can detect and locate, in the frequency

domain, very small deviations from normal operating conditions. Fractional deviation comparison detected abnormal signals 12.5 times smaller than the actual abnormal signal for LPRM instrument tubes impacting against channel boxes. The use of NRMS analysis would detect LPRM tube vibrations before damage occurred. NSP analysis, on a fractional deviation basis, would allow the abnormal signal to be classified as representing a LPRM impacting against a channel box, if a NSP portraying this impacting was available from the reference library of abnormal NSP's.

VII. FUTURE WORK

Neutron noise data must be collected and analyzed on a routine basis. The first goal is to determine the length of time a NSP is valid, and the second goal is to establish a library of NSP for the full range of reactor operating conditions.

The monitoring procedure must be tested and modified to fit the reactor personnel and equipment requirements. Experience and baseline data must be gained to build confidence in neutron noise analysis. After this confidence is gained a system for continuous on-line monitoring should be designed to fit the reactor personnel and equipment abilities and then presented to the power plant management for acceptance.

For utility acceptance the neutron noise monitoring program must provide the maximum amount of data with the greatest amount of ease and the least expense. Future work should determine the number of detectors that need to be routinely examined. This work should be done to determine the number of detectors in a LPRM string that need to be monitored and the number of LPRM strings that need to be monitored.

VIII. LITERATURE CITED

1. American Nuclear Society. 1975. To inspect BWR's again; core vibrations sought. Nuc. News 18(8): 39.

2. Ando, Y., A. Tanabe, and N. Kitanua. 1975. Void detection in BWR by noise analysis. J. of Nuc. Sci. and Technol. 12: 67-69.

3. Atta, M. A., J. E. Mott, and D. N. Fry. 1976. Determination of void fraction in BWR's using neutron noise analysis. Am. Nuc. Soc. Trans. 23: 466-467.

4. Bendat, J. S., and A. G. Piersol. 1971. Random data: Analysis and measurement procedures. John Wiley & Sons, Inc., New York, N.Y. 407 pp.

5. Blomberg, P. E., and F. Akerhielm. 1975. A contribution to the experience of noise measurements and analysis in a BWR power plant. Annals of Nuclear Energy 2: 323-331.

6. Brigham, E. O., and R. E. Morrow. 1967. The fast Fourier transform. IEEE Spectrum 4(12): 63-70.

7. Cohn, C. E. 1960. A simplified theory of pile noise. Nuc. Sci. and Eng. 7: 472-475.

8. Fry, D. N., R. C. Kryter, and J. C. Robinson. 1975. Analysis of neutron-density oscillations resulting from core barrel motions in a PWR nuclear power plant. Annals of Nuclear Energy 2: 341-351.

9. Fry, D. N., J. C. Robinson, R. C. Kryter, and O. C. Cole. 1975. Core component vibration monitoring in BWR's using neutron noise. Am. Nuc. Soc. Trans. 22: 623-624.

10. Fry, D. N. 1971. Experience in reactor malfunction diagnosis using on-line noise analysis. Nuc. Technol. 10: 273-282.

11. Gonzalez, R. C., D. N. Fry, and R. C. Kryter. 1974. Results in the application of pattern recognition methods to nuclear reactor core component surveillance. IEEE Trans. Nuc. Sci. 21(1): 750-756.

12. Harris, R. T. 1976. Investigations of an in-core flux anomaly in an operating BWR. Am. Nuc. Soc. Trans. 23: 464-465.

13. Holthaus, K. C. 1976. Application of neutron noise analysis and pattern recognition techniques to in-core surveillance of nuclear reactors. M.S. thesis. Iowa State University. 123 pp.

14. Kryter, R. C. 1969. Application of the FFT algorithm to on-line reactor diagnosis. IEEE Trans. Nuc. Sci. 16: 210-213.

15. Lewis, R. H., V. C. McAdams, and J. R. Penland. 1973. Neutron noise measurements at Oconee I. Am. Nuc. Soc. Trans. 17: 378-379.

16. Mathis, M. V., C. M. Smith, D. N. Fry, and M. L. Dailey. 1977. Characteristic studies of BWR-4 neutron noise analysis spectra. Am. Nuc. Soc. Trans. 27: 677-678.

17. Mathis, M. V., D. N. Fry, J. C. Robinson, and J. E. Jones. 1976. Neutron noise measurements to evaluate BWR-4 core modifications to prevent instrument tube vibration. Am. Nuc. Soc. Trans. 23: 466.

18. Mott, J. E., J. C. Robinson, D. N. Fry, and M. P. Braklin. 1976. Detection of impacts of instrument tubes against channel boxes in BWR-4's using neutron noise analysis. Am. Nuc. Soc. Trans. 23: 465.

19. Nabavian, M. 1977. Interpretation of neutron noise spectra measured in the presence of fluctuating voids. Ph.D. thesis. Iowa State University. 145 pp.

20. Otnes, R. K., and L. Enockson. 1972. Digital time series analysis. John Wiley & Sons, Inc., New York, N.Y. 467 pp.

21. Piety, K. R., and J. C. Robinson. 1975. An on-line reactor surveillance algorithm based on multivariate analysis of noise. Pages 15-1-15-33 in T. W. Kerlin, ed. Power Plant Dynamics Control and Testing Symposium. University of Tennessee, Knoxville, Tenn.

22. Robinson, J. C., and J. E. Mott. 1973. Nuclear power plant noise monitoring. Am. Nuc. Soc. Trans. 17: 376-377.

23. Seifritz, W., and D. Stegeman. 1971. Noise analysis in reactors at power. Atomic Energy Review 9(1): 163-175.

24. Thie, J. A. 1968. Noise in power reactors — A review of experiment, analysis, and theory. Reactor and Fuel-Processing Technology 11(4): 167-171.

25. Thie, J. A. 1972. Reactor-noise monitoring for malfunction. Reactor Technol. 14(4): 354-365.

26. Uhrig, R. E. 1973. State of the art of noise analysis in power reactors. CONF-730304.

IX. ACKNOWLEDGMENTS

The author expresses a great deal of thanks to his major professor, Dr. R. A. Hendrickson. Without his knowledge of the subject, insight of the problem, and his gentle nudging this study would not have come into being. Anyone who has done graduate work knows how inadequate these few words are.

The financial support and technical services supplied by the Iowa State University Engineering Research Institute and the Affiliate Research Program in Electrical Power were extremely instrumental in the success of this study. The ALRR staff and the Chemical Engineering and Nuclear Engineering Department's reactor technician, Elden Plettner, have my appreciation for services rendered.

A special thanks goes to the Duane Arnold Energy Center engineering staff for technical and spiritual support during data acquisition.

X. APPENDIX A.

NORMALIZATION PROCEDURES

Normalization of the raw PSD's, calculated using the PDP-15, is very important because this normalization enables NPSD's from reactors of similar design to be compared. The frequency (f_k) dependent normalization used in this study consisted of seven factors:

1. Analog to digital conversion factor, $A_a = (10/2048)$
2. Window function attentuation, $A_w = (1/0.5)$
3. Transformation factor, $A_t = 2/(N \cdot f_s)$
4. Calibration factor of FFT program, K
5. Filter attentuation, $1/X(f_k)$
6. Total gain A_T applied to the signal squared, $1/A_T^2$
7. Mean value $\bar{V}$ of the time domain data signal squared, $1/\bar{V}^2$.

Factors 1-4 are constants for each channel for the A-D converter, A and B. The first factor, A-D conversion, is a specification for the converter and is $2.38(10^{-5})$. Both channels of the converter are the same. The window function correction (20) is 1/0.5 and the transformation factor (4) is $2/(512 \cdot 25.6)$ or $1.53(10^{-4})$.

The calibration of the FFT program yielded different constants for each channel of the A-D converter. The first step of this calibration was to find the frequency at which the filter of the A-D converter had a gain of unity. Then a white noise generator, Hewlett Packard model 3722A, producing a 0.02 ($volts^2$) PSD, over the 0-500 HZ range, was input to the analysis equipment. The FFT output at the frequency where the filter gain equals 1.0 was then multiplied by the factor needed to obtain a

$0.02\ (\text{volts})^2$ value or

$$0.02 = K(Y_{FFT})$$

where Y_{FFT} is the PSD value from the FFT output and K is the calibration factor of the FFT program. Therefore,

$$K = 0.02/Y_{FFT}.$$

Channel A of the A-D converter has a K_A of $2.98(10^5)$ and channel B has a K_B of $3.79(10^5)$.

The total conversion factors of combining 1-4 in the previous list are channel A-$2.17(10^{-3})$, channel B-$2.76(10^{-3})$.

The filter attenuation is a set of correction factors corresponding to the frequency ranges used in calculating the NPSD's. The noise generator signal was input to the analysis equipment and the output of the FFT program was normalized to the value corresponding to the frequency at which the filter had been proven to have a gain of unity. The appropriate frequency ranges of the PSD's were then divided by the corresponding filter attenuation factor during normalization. The set of filter attenuation factors follows:

Filter Attenuation Factors

X_A	X_B	f_k(Hz)
0.7510E 00	0.9310E 00	0.1500E 00
0.8720E 00	0.1080E 01	0.4000E 00
0.1004E 01	0.1243E 01	0.6500E 00
0.8630E 00	0.1074E 01	0.9000E 00
0.8060E 00	0.1001E 01	0.1150E 01
0.7430E 00	0.9240E 00	0.1400E 01
0.8320E 00	0.1037E 01	0.1650E 01
0.7800E 00	0.9690E 00	0.1900E 01

X_A	X_B	f_k(Hz)
0.9490E 00	0.1181E 01	0.2150E 01
0.8810E 00	0.1097E 01	0.2400E 01
0.1017E 01	0.1227E 01	0.2650E 01
0.8150E 00	0.1012E 01	0.2900E 01
0.1007E 01	0.1250E 01	0.3150E 01
0.1064E 01	0.1287E 01	0.3400E 01
0.1007E 01	0.1224E 01	0.3650E 01
0.8770E 00	0.1090E 01	0.3900E 01
0.9540E 00	0.1208E 01	0.4150E 01
0.9720E 00	0.1213E 01	0.4400E 01
0.1142E 01	0.1727E 01	0.4650E 01
0.1074E 01	0.1337E 01	0.4900E 01
0.1040E 01	0.1293E 01	0.5150E 01
0.1052E 01	0.1310E 01	0.5400E 01
0.1118E 01	0.1394E 01	0.5650E 01
0.1319E 01	0.1642E 01	0.5900E 01
0.1134E 01	0.1399E 01	0.6150E 01
0.1090E 01	0.1340E 01	0.6400E 01
0.1335E 01	0.1655E 01	0.6650E 01
0.1280E 01	0.1585E 01	0.6900E 01
0.1302E 01	0.1612E 01	0.7150E 01
0.1383E 01	0.1699E 01	0.7400E 01
0.1345E 01	0.1642E 01	0.7650E 01
0.1570E 01	0.1905E 01	0.7900E 01
0.1465E 01	0.1755E 01	0.8150E 01
0.1446E 01	0.1707E 01	0.8400E 01
0.1536E 01	0.1783E 01	0.8650E 01
0.1236E 01	0.1414E 01	0.8900E 01
0.1169E 01	0.1308E 01	0.9150E 01

$\bar{V}$ and A_T were variables dependent on the data signal being processed. $\bar{V}$ and A_T can best be understood by studying Fig. 23. To obtain these two values required planning and designing during construction of SPARTAN, use of the tape recorder, writing of data acquisition procedures, and analysis of data to produce NPSD's. Once all the required information is obtained then $\bar{V}$ and A_T can be calculated using

$$\bar{V} = \frac{S_{ave}}{A_a A_f A_r} - \frac{V_a}{A_f A_r} - \frac{V_f}{A_r} - V_b$$

and

$$A_T = A_r A_f$$

The normalization of CPSD's included the same factors as above but required modification of factors four and five because two channels are involved with the CPSD calculation. The FFT calibration factor for CPSD's is

$$K_C = (K_A K_B)^{1/2}$$

where K_A and K_B are the FFT calibration factors of channel A and B respectively. The filter attenuation factor $X_C(f_k)$ for CPSD's is given by

$$X_C(f_k) = (X_A X_B)^{1/2}$$

where X_A and X_B are the filter attenuation factors for channels A and B respectively.

For example, the total normalization factor for channel A at 3.15 Hz with a $\bar{V}$ of 3 volts and a A_T of 5 is:

$$N_T(f_k) = (A_a)^2 (A_t)(A_w)(K_A)\left(\frac{1}{X_A}\right)\left(\frac{1}{\bar{V}^2}\right)\left(\frac{1}{A_T^2}\right)$$

$$N_T(3.15) = \left(\frac{10}{2048}\right)^2 \left(\frac{2.0}{(512)(256)}\right)\left(\frac{1}{0.5}\right)[2.98(10^5)]\left(\frac{1}{1.007}\right)\left(\frac{1}{3^2}\right)\left(\frac{1}{5^2}\right)$$

$$N_T(3.15) = 9.57(10^{-6})$$

The NPSD is then calculated as

$$NPSD(f_k) = PSD(f_k)\ N_T(f_k)$$

The following is the program used to normalize raw PSD's.

```
C          THE PURPOSE OF THIS PROGRAM IS TO CALCULATE NORMALIZED
C     POWER SPECTRAL DENSITIES(NPSD), NORMALIZED CROSS POWER
C     SPECTRAL DENSITIES(NCPSD), COHERENCE(COHEN), AND PHASE FUNCTIONS.
C     NPSD,NCPSD,COHEN,AND PHAES VALUES ARE PRINTED WITH THEIR
C     CORRESPONDING FREQUENCY AND GRAPHED.  NPSD VALUES ARE PUNCHED OUT
C     ON DATA CARDS WITH A BLANK CARD SEPARATING DIFFERENT DATA SETS.
C     THE PROGRAM HAS SAMPLE CHARACTER AND CALL GRAPH STATEMENTS AND
C     YOU SHOULD INSERT YOUR OWN DESIRED STATEMENTS INTO THESE
C     POSITIONS.
C          THE PROGRAM CAN ACCOMODATE UP TO 200 FREQUENCY POINTS AND
C     AS MANY DATA SETS AS YOU WISH.
C          THE CONSTANTS USED IN THE PROGRAM ARE
C             1.  FF=CORRECTION FACTOR FOR WINDOW FUNCTION APPLIED TO
C                 DATA,A-D CONVERSION FACTOR, FFT PROGRAM CALIBRATION,
C                 AND TRANSFROMATION FACTOR.
C             2.  FE=SAME AS FF BUT FOR DIFFERENT ANALZYER CHANNEL.
C          THESE TWO VALUES WILL HAVE TO BE CHANGED.
C        INPUT
C     N=NUMBER OF FREQUENCY POINTS AVERAGED OR SMOOTHED TOGETHER.
C     M=NUMBER OF FREQUENCY POINTS AFTER SMOOTHING OF ORIGINAL DATA.
C     AFREQ=FREQUENCY INCREMENT OF NPSD, NCPSD, AND COHEN AFTER
C     SMOOTHUNG.
C     FREQ(1)=FIRST FREQUENCY POINT OF NPSD,ETC. AFTER SMOOTHING.
C     MM=NUMBER OF FREQUENCY POINTS IN ORIGINAL DATA.
C     CI(I)=ARRAY OF FILTER ATTENUATION FACTORS CORRESPONDING TO THE
C     FREQUENCY POINTS AFTER SMOOTHING.
C     F(I)=SAME AS CI(I) BUT FOR DIFFERENT ANALYZER CHANNEL.
C     A(I)=PSD FOR CHANNEL A OF ANALYZER.
C     B(I)=SAME AS A(I) BUT FOR CHANNEL B.
C     PR(I)= REAL PART OF CPSD.
C     PI(I)=IMAGINARY PART OF CPSD.
C     BFREQ(I)=FREQUENCY POINT ARRAY BEFORE SMOOTHING.
C     VA=MEAN VOLTAGE OF DATA SIGNAL IMPUT TO CHANNEL A.
C     VB=MEAN VOLTAGE OF DATA SIGNAL INPUT TO CHANNEL B.
C     AG=TOTAL GAIN APPLIED TO DATA SIGNAL FOR CHANNEL A.
```

```
C      BG=TOTAL GAIN APPLIED TO DATA SIGNAL FOR CHANNEL B.
       DIMENSION A(200),B(200),CR(200),CI(200),NCPSD(200),NAPSD(200),
      1NBPSD(200),F(200),COHEN(200),WNA(200),WNB(200),FREQ(200),
      1PR(200),PI(200),PHASE(220),CO(200),BFREQ(200)
       REAL NAPSD,NBPSD,NCPSD
       CHARACTER*20 XL/' FREQUENCY,HERTZ '/,YL/'      NPSD(HZ-1)      '/,
      1DAT/' P/F=100/100   77286'/,YLO/'     NCPSD(HZ-1)      '/,
      1GA/' DAEC 253   40-25-D '/,GLA/' DAEC 253   40-25-A'/,
      1GLO/' DAEC 253 40-25 A/D '/,YLT/'     COHERENCE       '/,
      1GB/' DAEC 253   40-25-C '/,GLB/' DAEC 253   40-25-B'/,
      1GC/' DAEC 251   40-25-D '/,GLC/' DAEC 251   40-25-A'/,
      1GD/' DAEC 251   40-25-C '/,GLD/' DAEC 251   40-25-B'/,
      1GE/' DAEC 252   40-25-D '/,GLE/' DAEC 252   40-25-A'/,
      1GL/' DAEC 252   40-25-C '/,GLT/' DAEC 252   40-25-B'/,
      1GLP/' DAEC 253 40-25 B/C '/,
      1GLQ/' DAEC 251 40-25 A/D '/,
      1GLU/' DAEC 252 40-25 A/D '/,
      1GLV/' DAEC 252 40-25 B/C '/,
      1GLR/' DAEC 251 40-25 B/C '/,
      1GLZ/' DAEC 253 40-25 B/D '/,
      1GLX/' DAEC 253 40-25 C/D '/,
      1GLY/' DAEC 251 40-25 B/D '/,
      1GLW/' DAEC 252 40-25 B/D '/,
      1GLL/' DAEC 252 40-25 C/D '/,
      1GLM/' DAEC 251 40-25 C/D '/,
      1YLTR/'        PHASE          '/
        READ,N,M,AFREQ,FREQ(1),MM
       FF=2.167E-3
       FE=2.755E-3
       FG=2.443E-3
       DO 20 I=1,M
       READ55,CI(I),F(I)
       WNA(I)=(SQRT(CI(I)))*(SQRT(F(I)))
   55  FORMAT(2F5.4)
   20  CONTINUE
```

```
      DO 80 I=2,M
   80 FREQ(I)=FREQ(I-1)+AFREQ
      DO 99 NN=1,3
      READ,VA,VB,AG,BG
      DO 1 I=1,MM
      READ40,A(I),B(I),PR(I),PI(I),BFREQ(I)
   40 FORMAT(F10.3,F9.3,F9.3,F9.3,F5.2)
    1 CONTINUE
      DO 90 I=2,MM
   90 IF(PR(I).EQ.0.)PR(I)=(PR(I-1)+PR(I+1))/2
      PRINT91
   91 FORMAT(' ',' PHASE ANGLE  ',4X,'  FREQUENCY  ')
      DO 10 I=1,MM
      NCPSD(I)=SQRT((PR(I)**2)+(PI(I)**2))
      CO(I)=(NCPSD(I)**2)/(A(I)*B(I))
C     CALCULATING PHASE ANGLE
      PHASE(I)=(180./3.1416)*ATAN(PI(I)/PR(I))
      IF(PI(I).GT.0..AND.PR(I).GT.0.)PHASE(I)=PHASE(I)-360.
      IF(PI(I).GT.0..AND.PR(I).LT.0.)PHASE(I)=PHASE(I)-180.
      IF(PI(I).LT.0..AND.PR(I).LT.0.)PHASE(I)=PHASE(I)-180.
      PRINT,PHASE(I),BFREQ(I)
   10 CONTINUE
      DO 11 J=1,M
      CR(J)=0.0
      L=((J-1)*N)+1.0
      LL=L+N-1.0
      DO 12 K=L,LL
      CR(J)=CR(J)+(NCPSD(K)/N)
   12 CONTINUE
   11 CONTINUE
      DO 13 J=1,M
      NAPSD(J)=0.0
      NBPSD(J)=0.0
      COHEN(J)=0.
      L=((J-1.0)*N)+1.0
```

```
      LL=L+N-1.0
C     CALCULATING NAPSD,NBPSD,NCPSD,AND COHEN.
      DO 14 K=L,LL
      NAPSD(J)=NAPSD(J)+(A(K)/N)
      NBPSD(J)=NBPSD(J)+(B(K)/N)
      COHEN(J)=COHEN(J)+(CO(K)/N)
   14 CONTINUE
      NAPSD(J)=(NAPSD(J)*FF)/(CI(J)*((VA*AG)**2))
      NBPSD(J)=(NBPSD(J)*FE)/(F(J)*((VB*BG)**2))
      NCPSD(J)=FG*CR(J)/(VA*VB*AG*BG*WNA(J))
      WRITE(7,50) NAPSD(J)
   50 FORMAT(E13.6)
   13 CONTINUE
      WRITE(7,49) NN
   49 FORMAT(I4)
      PRINT61
   61 FORMAT(' ',' NAPSD ',1X,' NBPSD ',1X,' NCPSD ',1X,
     1' COHEN ')
      DO 30 J=1,M
      WRITE(7,50) NBPSD(J)
      PRINT60,NAPSD(J),NBPSD(J),NCPSD(J),COHEN(J),FREQ(J)
   60 FORMAT(' ',E10.3,E10.3,E10.3,E10.3,F5.2)
      NAPSD(J)=ALOG10(NAPSD(J))
      NBPSD(J)=ALOG10(NBPSD(J))
      NCPSD(J)=ALOG10(NCPSD(J))
   30 CONTINUE
      WRITE(7,49) NN
C          THIS SET OF IF STATEMENTS SELECT THE GRAPHING LABELS FOR THE
C     DATA TO PLOTTED.  SUGGEST GRAPHING NO MORE DATA THAN THE
C     EQUIVALENCE OF 16 GRAPHS OF 37 POINTS AND 4 GRAPHS OF 200 POINTS.
      IF(NN.EQ.2) GO TO 98
      IF(NN.EQ.3) GO TO 97
      IF(NN.EQ.4) GO TO 96
      CALL GRAPH(M,FREQ,NAPSD,3,2,5.,-7.,2.,0.,5., -7.,XL,YL,GC,DAT)
      CALL GRAPH(M,FREQ,NBPSD,3,2,5.,-7.,2.,0.,5., -7.,XL,YL,GLD,DA)
```

```
      CALL GRAPH(M,FREQ,NCPSD,3,2,5.,-7.,2.,0.,5., -8.,XL,YLO,GLY,D)
      CALL GRAPH(M,FREQ,COHEN,3,2,5.,7.,2.,0.,.15,0.,XL,YLT,GLY,DAT)
      CALL GRAPH(200,BFREQ,PHASE,3,2,5.,7.,2.,0.,0.,0.,XL,YLTR,GL,D)
      GO TO 99
98    CALL GRAPH(M,FREQ,NAPSD,3,2,5.,-7.,2.,0.,5., -7.,XL,YL,GC,DAT)
      CALL GRAPH(M,FREQ,NBPSD,3,2,5.,-7.,2.,0.,5., -7.,XL,YL,GD,DAT)
      CALL GRAPH(M,FREQ,NCPSD,3,2,5.,-7.,2.,0.,5., -8.,XL,YLO,GLM,D)
      CALL GRAPH(M,FREQ,COHEN,3,2,5.,7.,2.,0.,.15,0.,XL,YLT,GLM,DAT)
      CALL GRAPH(200,BFREQ,PHASE,3,2,5.,7.,2.,0.,0.,0.,XL,YLTR,GL,D)
      GO TO 99
97    CALL GRAPH(M,FREQ,NAPSD,3,2,5.,-7.,2.,0.,5., -7.,XL,YL,GE,DAT)
      CALL GRAPH(M,FREQ,NBPSD,3,2,5.,-7.,2.,0.,5., -7.,XL,YL,GLT,DA)
      CALL GRAPH(M,FREQ,NCPSD,3,2,5.,-7.,2.,0.,5., -8.,XL,YLO,GLW,D)
      CALL GRAPH(M,FREQ,COHEN,3,2,5.,7.,2.,0.,.15,0.,XL,YLT,GLW,DAT)
      CALL GRAPH(200,BFREQ,PHASE,3,2,5.,7.,2.,0.,0.,0.,XL,YLTR,GL,D)
      GO TO 99
96    CALL GRAPH(M,FREQ,NAPSD,3,2,5.,-7.,2.,0.,5., -7.,XL,YL,GL,DAT)
      CALL GRAPH(M,FREQ,NBPSD,3,2,5.,-7.,2.,0.,5., -7.,XL,YL,GLT,DA)
      CALL GRAPH(M,FREQ,NCPSD,3,2,5.,-7.,2.,0.,5., -8.,XL,YLO,GLV,D)
      CALL GRAPH(M,FREQ,COHEN,3,2,5.,7.,2.,0.,.15,0.,XL,YLT,GLV,DAT)
      CALL GRAPH(200,BFREQ,PHASE,3,2,5.,7.,2.,0.,0.,0.,XL,YLTR,GL,D)
99    CONTINUE
      STOP
      END
```

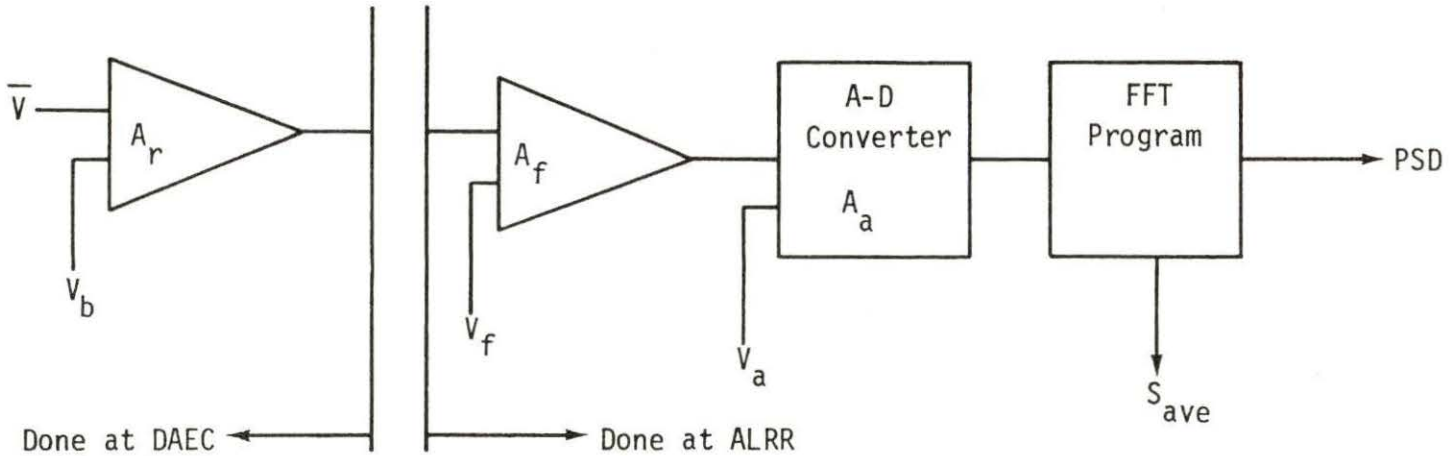

$\overline{V}$ = mean value of data signal
V_b = bias applied at the reactor site
A_r = gain of SPARTAN and FM tape recorder
V_f = bias applied as final conditioning of data signal
A_f = gain applied as final conditioning of data signal
V_a = internal bias of converter
A_a = conversion factor for converter
S_{ave} = mean value of the signal input to the FFT program

Figure 23. Conditioning of data signal mean value

XI. APPENDIX B.

PDP-15 PROCEDURE FOR THE COMPUTATION OF SPECTRA

The procedure for the computation of spectra from time series data is given in this appendix. The system was capable of analyzing two signals simultaneously which allowed the power spectral density (PSD) of each signal, the cross power spectral density (CPSD), the coherence, and phase lag between the two signals to be calculated.

The limited amount of memory in the ALRR PDP-15 computer limited the number of time domain data points, N, to 512 words for each of the two signals being analyzed. The filter of the A-D converter was set at an upper cutoff frequency of 10 Hz and a sampling rate, f_s, set at 25.6 samples per second.

The Nyquist frequency (f_c) is given by

$$f_c = \frac{f_s}{2} = 12.8 \text{ Hz} \tag{10}$$

and the discrete spectral points are separated by the resolution bandwidth given by

$$B_e = \frac{f_s}{N} = 0.05 \text{ Hz} \tag{11}$$

The discrete frequency points of the spectra are

$$f_k = \frac{kf_s}{N} \text{ , } k = 0, 1, 2, 3 \ldots N - 1 \tag{12}$$

Therefore, f_k = 0, 0.05, 0.1, 0.15, ... 25.55 Hz but, f_c = 12.8 Hz which shows that unique results are obtained only for k = 0, 1, 2, 3, ... N/2 - 1. The discrete frequency points then become 0, 0.05, 0.1,

0.15 ... 12.8 Hz.

The PDP-15 program first calculates the mean value of the time signal and subtracts this mean value from all data points. The second step is to apply a window function to the data to reduce the side-lobe leakage. The window used was a complete cosine squared function (20) given by

$$w(t) = \cos^2 \frac{\pi t f_s}{N} \quad , \quad t = \pm \frac{n}{f_s} \quad , \quad n = 0, 1, 2, 3 \ldots \frac{N}{2} - 1 \qquad (13)$$

The Fourier transform of the two time domain signals is now computed by inserting one record x(n) as the real part and one record y(n) as the imaginary part of the complex record z(n)

$$z(n) = x(n) + iy(n) \qquad (14)$$

and z(n) is Fourier transformed to Z(k), k = 0, 1, 2, ... N - 1, using the FFT algorithm. The Fourier transforms of x(n) and y(n) are given as

$$X(k) = \frac{Z(k) + Z^*(N - k)}{2} \qquad (15)$$

and

$$Y(k) = \frac{Z(k) - Z^*(N - k)}{2} \qquad (16)$$

where

$$Z(k) = e(k) + if(k). \qquad (17)$$

and the Nyquist cut-off frequency occurs when k = N/2, giving unique results only when k = 0, 1, 2, ... N/2 - 1. The raw estimates of the PSD's are

$$\tilde{G}_x(k) = |X(k)|^2 \tag{18}$$

and

$$\tilde{G}_y(k) = |Y(k)|^2 \tag{19}$$

Using Eqs. (15), (16), and (17)

$$\tilde{G}_x(k) = a^2(k) + b^2(k) \tag{20}$$

and

$$\tilde{G}_y(k) = c^2(k) + d^2(k) \tag{21}$$

where

$$a(k) = [e(k) + e(N - k)]/2 \tag{22}$$

$$b(k) = [f(k) - f(N - k)]/2$$

$$c(k) = [f(k) + f(N - k)]/2 \tag{23}$$

and

$$d(k) = [e(N - k) - e(k)]/2 \tag{24}$$

The raw estimates of the real, $\tilde{C}_{xy}(k)$, and imaginary, $\tilde{Q}_{xy}(k)$ components of the CPSD function are given by

$$\tilde{C}_{xy}(k) = a(k)c(k) + b(k)d(k) \tag{25}$$

and

$$\tilde{Q}_{xy}(k) = b(k)c(k) - a(k)d(k) \tag{26}$$

The PDP-15 outputs the PSD of each data signal and the real and imaginary values of the CPSD. Normalization and calculation of CPSD, coherence,

and phase are done outside the PDP-15 program. The CPSD, coherence, and phase functions are calculated using

$$\text{CPSD}(k) = [\tilde{C}^2_{xy}(k) + \tilde{Q}^2_{xy}(k)]^{1/2} \tag{27}$$

$$\text{Coherence} = \text{CPSD}^2(k)/[\tilde{G}_x(k) \cdot \tilde{G}_y(k)] \tag{28}$$

and

$$\text{Phase} = \frac{180}{\pi} \tan^{-1}[\frac{\tilde{Q}_{wy}(k)}{\tilde{C}_{xy}(k)}]. \tag{29}$$

XII. APPENDIX C. DATA ACQUISITION PROCEDURES

This appendix contains the data acquisition procedure used by the DAEC engineering staff. Also included is a DATA LOG SHEET which was used to insure all necessary data were properly recorded or logged.

A. Outline of Procedures

The acquisition of data will be done three times a day at approximately 8:00 a.m., 12:00 (noon), and 4:00 p.m. The data acquisition is broken into two parts:

A. Calibrating and initializing equipment.

B. Recording data on FM tape recorder.

Calibrating and initializing the equipment will be done every morning (8:00 a.m.) before recording data and consists of:

A. Calibrating tape recorder.

B. Assuring tape recorder is in proper operating order.

C. Proper adjustment for signal conditioning.

The properly conditioned signal will then be recorded for three 20-minute periods. These data acquisitions will be recorded on the same tape, therefore the DATA LOG SHEET's for one day of data acquisition will have the same tape reel number (item 24). When this full data tape is removed from the recorder, it should be placed in the provided envelope along with the three DATA LOG SHEET's and other requested information. This envelope should then be sealed and labeled with the data tape number.

The Calibration Procedure is to be used for the 8:00 a.m. data acquisition and the Date Acquisition Procedure is to be used for the 12:00 and 4:00 acquisitions.

B. Calibration Procedure

TR = Four Channel Tape Recorder

SPARTAN = Signature Pattern Acquisition from Reactor Amplified Noise

1. Remove tape reel presently on TR. Thread calibration tape as shown by lines on tape compartment.
2. Set tape speed at 3.75 ips on TR
3. Place ON/OFF switch of the record/reproduce module on TR in ON position for channels 1-4. FREQ/PHASE should be in FREQ.
4. Set OUTPUT CUTOFF switch (red knob) of TR at 1 kHz for channels 1-4.
5. Check for proper tape threading. The tape must be tight.
6. Set FM/DIRECT selector switch (black knob) on TR to FM for channels 1-4. NEVER USE DIRECT.
7. Set INPUT GAIN fully counter-clockwise, using the provided screwdriver.
8. Press and hold RECORD pushbutton on TR; press STOP pushbutton; release STOP and then release RECORD. Four red lights should come on.
9. Calibrate Digital Volt Meter (DVM)
   A. Press Zero DVM of TAPE REC SELECT pushbutton set on SPARTAN. Adjust DVM to 00.0 and the sign toggling

between + and -.

B. Press Read Cal Sig of TAPE REC SELECT pushbutton set. Adjust DVM to 1727 ± 2.

C. Repeat A and B until desired conditions are met.

10. Press Tape Rec Cal of FUNCTION SELECT pushbutton set and Ch 1 of TAPE REC SELECT pushbutton set on SPARTAN.

11. Press STOP pushbutton on TR.

12. Set FM/DIRECT selector switch (black knob) of record/reproduce module of TR to FM ZERO for channels 1-4. Four green lights should come on.

13. Log the desired information for items 1-7 and 12-15 on DATA LOG SHEET. See COMMENT #4 at end of procedures.

14. Adjust OUTPUT ZERO for channel #1 on TR to 000 ± 100 on the DVM on SPARTAN. Repeat for TR channels 2-4 by selecting Ch 2, Ch 3, and Ch 4 of TAPE REC SELECT pushbutton set on SPARTAN.

15. Press and hold RECORD pushbutton on TR; press forward (▷) DRIVE pushbutton; release RECORD and DRIVE. Four red lights should come on. Let TR run for five minutes before going to step 16.

16. Press Ch 1 of TAPE REC SELECT on SPARTAN. Adjust INPUT ZERO for channel #1 on TR to 000 ± 200 on the DVM on SPARTAN. Repeat for TR channels 2-4 by selecting Ch 2, Ch 3, and Ch 4 of TAPE REC SELECT pushbutton set on SPARTAN. There will be a time lag between adjustment and readout on DVM.

17. Set FM/DIRECT selector switch (black knob) of record/reproduce module on TR to FM GAIN CAL for channels 1-4.

18. Press Ch 1 of TAPE REC SELECT pushbutton set on SPARTAN and observe the signal on the oscilloscope. The signal should be a sine wave. The monitor meter for TR channel #1 should read approximately 1 volt. If the above conditions are met then channel #1 of the TR is in proper operation. If the above signals are not obtained press the STOP pushbutton on TR. Switch the FM/DIRECT selector (black knob) to FM and then back to FM GAIN CAL. Switch the OUTPUT CUTOFF switch (red knob) to 100 cps and then back to 1 kHz. If the sine wave and the 1 volt reading are obtained then TR channel #1 is in proper operating condition. In case of channel failure see COMMENT #1 at end of procedures.
19. Repeat step 17 for TR channels 2-4 by selecting Ch 2, Ch 3, and Ch 4 of TAPE REC SELECT pushbutton set on SPARTAN. Log desired information for items 8-11 on DATA LOG SHEET for each data acquisition.
20. Press First Bias Adj. of FUNCTION SELECT pushbutton set and BIAS 1 of BIAS SELECT pushbutton set on SPARTAN.
21. Set bias #1, as read on DVM, opposite in sign and equal to the mean DC level of the LRPM signal input to channel #1, this is the value entered on item #12 on the DATA LOG SHEET. Adjust bias #1 using pot on front of SPARTAN. See Fig. 3.4.
22. Repeat steps 21 and 22 using Bias 2, Bias 3, and Bias 4 of BIAS SELECT pushbutton set on SPARTAN and items 13-15 on DATA LOG SHEET.

23. Set FM/DIRECT selector switch (black knob) to FM for TR channels 1-4.
24. Adjust INPUT GAIN of channels 1-4 on TR until white dots line up.
25. Adjust GAIN pots on SPARTAN to read 250 for channels 1-4.
26. Press Final Bias & Gain Adj of FUNCTION SELECT pushbutton set on SPARTAN.
27. Press Ch 1 of TAPE REC SELECT pushbutton set on SPARTAN.
28. Adjust gain and bias of channel #1 on SPARTAN to get the proper signal on the oscilloscope. The proper signal is 2 volts peak-to-peak and centered around zero. See Fig. 3.5.
29. Repeat steps 27 and 28 using Ch 2, Ch 3, and Ch 4 of TAPE REC SELECT pushbutton set on SPARTAN.
30. Observe the data signals on the oscilloscope, using Ch 1, Ch 2, Ch 3, and Ch 4 of TAPE REC SELECT pushbutton set on SPARTAN, for 5 minutes per channel. This is to check for signals exceeding the 2 volt peak-to-peak level. If any such signals are observed reduce gain accordingly. See COMMENT #2 at end of procedures.
31. Log the desired information on items 16-23 on DATA LOG SHEET.
32. Press the STOP pushbutton on TR. Remove the calibration tape and thread a new data acquisition tape.
33. Log desired information for item 24 on DATA LOG SHEET. See COMMENT #4 at end of procedure.
34. Set the tape footage counter reading on TR to 0000.

35. Press and hold RECORD pushbutton on TR; press forward (▷) DRIVE pushbutton; release RECORD and DRIVE.

36. Press Bias Data of FUNCTION SELECT pushbutton set on SPARTAN. Log on DATA LOG SHEET the tape footage counter reading when Bias Data was activated, item #25. Let the TR run 10 ft before proceeding to step 37.

37. Press Acq Data of the FUNCTION SELECT pushbutton set on SPARTAN. Log tape footage counter reading when Acq Data was activated, item #26 on DATA LOG SHEET.

38. Log the final bias reading for channel #1. The bias is read on the DVM by activating Bias 1 of the BIAS SELECT pushbutton set on SPARTAN. Repeat for channels 2-4. Use items 27-30 on DATA LOG SHEET.

C. Data Acquisition Procedure

TR = Four Channel Tape Recorder

SPARTAN = Signature Pattern Acquisition from Reactor Amplified Noise

1. Set tape speed at 3.75 ips on TR.
2. Place ON/OFF switch on TR in ON position for channels 1-4.
3. Set OUTPUT CUTOFF switch (red knob) of TR at 1 kHz for channels 1-4. FREQ/PHASE should be in FREQ.
4. Check for proper tape threading. The tape must be tight.
5. Set FM/DIRECT selector (black knob) on TR to FM for channels 1-4.

6. Set gain and bias pots for channels 1-4 to values entered in items 16-23 on previous DATA LOG SHEET.
7. Press Final Gain & Bias Adj of FUNCTION SELECT pushbutton set on SPARTAN.
8. Log the desired information for items 1-15 and item 24 on DATA LOG SHEET.
9. Press and hold RECORD pushbutton on TR; press forward (▷) DRIVE pushbutton; release RECORD and DRIVE.
10. Briefly observe the four channels of data acquisition on the oscilloscope using Ch 1, Ch 2, Ch 3, and Ch 4 of TAPE REC SELECT pushbutton set on SPARTAN. The signals should be 2 volts peak-to-peak and centered around zero. See COMMENT #3 at end of procedures.
11. Press Bias Data of FUNCTION SELECT pushbutton set on SPARTAN. Log on DATA LOG SHEET (item #25) the tape footage counter reading when Bias Data was activated. Let TR run for 10 ft.
12. Press Acq Data of the FUNCTION SELECT pushbutton set on SPARTAN. Log tape footage counter reading (item #26) when Acq Data was activated.
13. Log the final bias reading for channel #1. The bias is read on the DVM by activating Bias 1 of the BIAS SELECT pushbutton set on SPARTAN. Repeat for channels 2-4. Use items 27-30 on DATA LOG SHEET.
14. Log the desired information on items 16-23 on DATA LOG SHEET.

D. Comments

1. The LPRM string to be used is 40-25. Signal connections are as follows:

   Channel 1 – 40-25-A

   Channel 2 – 40-25-B

   Channel 3 – 40-25-C

   Channel 4 – 40-25-D

   40-25-D and 40-25-C are the most important data signals. If the TR channel being used for the 40-25-C or 40-25-D signal becomes inoperative use the TR channel being used for the 40-25-A or 40-25-B signal.

2. The signal must be properly conditioned at this point because there will not be enough tape available to do so later. It is better to have the gain too low than too high.

3. This step (10 of DATA ACQUISITION) must be performed in one minute or less. If you have to make adjustments that take more time than this press STOP pushbutton on TR. Record the tape footage counter reading (on scrap of paper). Repeat step 9 and make necessary adjustments. After adjustments are made press FAST (◁) reverse pushbutton on TR and returned to the tape footage counter reading recorded above. Then proceed with step 10.

4. On the first day of each week of data acquisition a TIP trace should be obtained for the 40-25 LPRM string. This TIP Trace should be put with the first day's tape of data.

E. DATA LOG SHEET

When an item of information is logged check the box pertaining to that item at the right hand edge of the sheet.

1. Site of collection - _____ - /___/

2. Date - _____ - /___/

3. Operating conditions of reactor when data were collected, obtain P-1 Program output and rod position map --------- /___/

4. LPRM connected to channel #1 - _____ - /___/

5. LPRM connected to channel #2 - _____ - /___/

6. LPRM connected to channel #3 - _____ - /___/

7. LPRM connected to channel #4 - _____ - /___/

8. Channel #1 operable? YES NO (circle one) --------- /___/

9. Channel #2 operable? YES NO (circle one) --------- /___/

10. Channel #3 operable? YES NO (circle one) --------- /___/

11. Channel #4 operable? YES NO (circle one) --------- /___/

12. Mean DC level of LPRM signal connected to channel #1 - _____ - /___/

13. Mean DC level of LPRM signal connected to channel #2 - _____ - /___/

14. Mean DC level of LPRM signal connected to channel #3 - _____ - /___/

15. Mean DC level of LPRM signal connected to channel #4 - _____ - /___/

16. Channel #1 gain adjustment reading - _____ - /___/

17. Channel #2 gain adjustment reading - _____ - /___/

18. Channel #3 gain adjustment reading - _____ - /___/

19. Channel #4 gain adjustment reading - _____ - /___/

20. Channel #1 bias adjustment reading - _____ - /___/

21. Channel #2 bias adjustment reading - _____ - /___/

22. Channel #3 bias adjustment reading - _____ - /___/

23. Channel #4 bias adjustment reading - _____ - /___/

24. Magnetic tape reel number - _____ - /___/

25. Bias data activated - _____ - /___/

26. Acq data activated - _____ - /___/

27. Final bias voltage for channel #1 - _____ - /___/

28. Final bias voltage for channel #2 - _____ - /___/

29. Final bias voltage for channel #3 - _____ - /___/

30. Final Bias voltage for channel #4 - _____ - /___/

Double check the column of boxes at the right edge of these pages. There must be a check in EVERY BOX.